J 20 419 F

VHF COMMUNICATIONS

A PUBLICATION FOR THE RADIO AMATEUR
ESPECIALLY COVERING VHF, UHF AND MICROWAVES

VOLUME NO. 4 EDITION 4 NOVEMBER 1972 DM 4.00

VHF COMMUNICATIONS

Published by:
Verlag UKW-BERICHTE, Hans J. Dohlus oHG, 8520 Erlangen, Gleiwitzer Str. 45
Fed. Rep. of Germany. Tel. (0 91 31) 3 33 23 and (0 91 35) 4 07

Publishers:
T. Bittan, H. Dohlus, R. Lentz at equal parts

Editors:
Terry D. Bittan, G3JVQ/DJ0BQ, responsible for the text
Robert E. Lentz, DL3WR, responsible for the technical contents and layout

Advertising manager:
T. Bittan, Tel. (09191) – 3148

VHF COMMUNICATIONS,
the international edition of the German publication UKW-BERICHTE, is a quarterly amateur radio magazine especially catering for the VHF/UHF/SHF technology. It is published in February, May, August and November. The subscription price is DM 14.00 or national equivalent per year. Individual copies are available at DM 4.00, or equivalent, each. Subscriptions, orders of individual copies, purchase of P. C. boards and advertised special components, advertisements and contributions to the magazine should be addressed to the national representative.

Printed in the Fed. Rep. of Germany by R. Reichenbach KG, 8500 Nuernberg, Krelingstr. 39

We would be grateful if you would address your orders and queries to your representative :

VERTRETUNGEN: **REPRESENTATIVES:**

Argentina	Miguel Zajelenczyc, Gral. Cesar Diaz 1932, Buenos Aires S 16
Austria	Hans J. Dohlus, DJ 3 QC, D-8520 ERLANGEN, Gleiwitzer Straße 45, see Germany
Australia	WIA, PO Box 67, East Melbourne 3002, Victoria
Belgium	E. Drieghe, ON 5 JK, B-9160 HAMME, Kapellestr. 10, Telefon (052) 49457, PCR 588111
Canada W. Prov.	Otto Meginbir, VE 6 OH, 1170 Bassett Cres. NW. Medicine Hat, Alb.
Denmark	Sven Jacobson, SM 7 DTT, Ornbogatan 1, S-21232 MALMO, Tel. 49 16 93, Postkto. København 14985
France	Christiane Michel, F 5 SM, F-89 PARLY, les Pillés, CCP PARIS 16.219-66
Finland	Eero Valio, OH 2 NX, 04740 SALINKÄÄ, Postgiro 4363 39-0 und Telefon 915/86 265
Germany	Verlag UKW-BERICHTE H. Dohlus oHG, D-8520 ERLANGEN, Gleiwitzer Str. 45, Telefon (0 91 31) 3 33 23 + (0 91 35) 4 07, Deutsche Bank Erlangen Kto. 476 325, Postscheck 304 55 Nürnberg
Holland	S. Hoogstraal, PA ø MSH, ALMELO, Oranjestraat 40, giro 137 2 282, telefon (05490) — 1 26 87
Italy	STE s.r.l. (I 2 GM) via maniago 15, I-20134 MILANO, Tel. 21 78 91, Conto Corrente Postale 3/44968
Luxembourg	P. Wantz, LX 1 CW, Télévision, DUDELANGE, Postscheckkonto 170 05
Norway	H. Theg, LA 4 YG, Ph. Pedersensv. 15, N 1324 LYSAKER pr. Oslo, Postgiro 31 6000
South Africa	Arthur Hemsley ZS 5 D, P.O. Box 64, POINT, Durban Tel. 31 27 27
New Zealand	E. M. Zimmermann, ZL 1 AGQ, P.O. Box 56, WELLSFORD, Tel: 80 24
Spain+Portugal	Julio A. Prieto Alonso, EA 4 CJ, MADRID-15, Donoso Cortès 58 5°-B, Tel. 243.83.84
Sweden	Sven Jacobson, SM 7 DTT, S-21232 MALMO, Ornbogatan 1, Tel. 491693, Postgiro 43 09 65
Switzerland	Hans J. Dohlus, DJ 3 QC, D-8520 ERLANGEN, Gleiwitzer Straße 45, see Germany
United Kingdom	Sim Weir GM 3 SAN, 19 Ellismuir Rd., BAILLIESTON, Glasgow G69 7HW, Scotland Tel. 041-771-0364
USA-East Coast	VHF COMMUNICATIONS Russ Pillsbury, K 2 TXB, & Gary Anderson, W 2 UCZ, 915 North Main St. JAMESTOWN, NY 14701, Tel. 716-664-6345
USA-Central	Bob Eide, WØENC, 53 St. Andrew, RAPID CITY, SD 57701, Tel. 605-342-4143
USA-West Coast	Darrel Thorpe, Circuit Specialists Co. Box 3047, SCOTTSDALE AZ 85257, Tel. 602-945-5437

A PUBLICATION FOR THE RADIO AMATEUR
ESPECIALLY COVERING VHF, UHF AND MICROWAVES
VOLUME NO. 4 EDITION 4 NOVEMBER 1972

R. L. Harrison VK 2 ZTB	VHF Transequatorial Propagation	194—206
Editors	Corrections and Improvements to the DC 6 HL SSB Transceiver	207
AMSAT Newsletter	OSCAR 6	208—211
H. J. Franke DK 1 PN	An Integrated Receiver System for AM, FM, SSB and CW	212—215
W. Schumacher DJ 9 XN	Dimensioning of Microstripline Circuits Part 2	216—228
F. Weingärtner DJ 6 ZZ	Further Development of the four-digit Frequency Counter	229—234
R. Görl DL 1 XX B. Rössle DJ 1 JZ	A Stable Crystal-Controlled Oscillator in the order of 10^{-7} for Frequency and Time Measurements	235—240
T. Bittan G 3 JVQ/DJ Ø BQ	Amateur Television Part 2	241—252

NOTES TO OUR READERS

We would like to apologize for the delay in material shipments during the summer months. This has been caused by the moving of our despatch dept. to new, larger premises. This was planned for August when we were supposed to be on holiday. Unfortunately, the new rooms were not ready and still had to be plastered and have the windows installed. After we had threatened all parties with legal proceedings, the rooms were finished and we were able to commence settling the backlog. The new premises have allowed us to expand and employ more staff than in the previous location. We hope that this will speed up the processing of all material orders and improve our service. Thank you for being so patient.

We would like to take this opportunity of wishing all readers a very Happy Christmas and a prosperous New Year. Please do not forget to resubscribe to VHF COMMUNICATIONS since we have some really outstanding articles coming.

VHF TRANSEQUATORIAL PROPAGATION
PART I

by Roger Lenned Harrison, VK 2 ZTB

(Published with kind permission of the Australian Magazine Amateur Radio)

INTRODUCTION

Reception of VHF signals over very long paths that cross more-or-less transversely to the equatorial zone have been reported on many occasions in the last 25 years. The frequencies involved are generally far in excess of the predicted MUF and signal strengths sometimes approach free-space values. Path lengths reported are usually greater than 5,000 km, with a few up to 18,000 km. These signals are generally regarded as having arrived by "anomalous" transequatorial propagation.

Throughout the remainder of this article the author uses the letters TEP to denote this form of propagation, dropping the word "anomalous" since it turns out that it is not so anomalous as was first thought.

1. A SHORT HISTORY

The first instances of intercontinental VHF contacts were reported in "QST" by Ed Tilton in "The World Above 60 MC", May and October 1947 (1), (2).

The discovery of TEP by Radio Amateurs did not receive a great deal of attention in the scientific world until the late 1950's and the IGY in 1957/58.

Contacts between Australia and Hawaii, Mexico and Argentina, and the U.S.A. and Peru were fairly common during the years 1947 to 1951. There was then a sharp decline during the sunspot minimum, but new reports began to appear again in 1955. The number of reports reached a maximum during 1957 to 1960 and again during 1968 to 1971. Some contacts were reported over extremely long paths, e.g. South Africa to England (13,000 km.), Buenos Aires to Western U.S.A. (9,860 km.), Argentina to Hawaii (12,150 km.), Argentina to Japan (18,760 km.), and Australia to Mexico (10,500 km.).

The first scientific paper to appear on the phenomena of TEP was by Ed Tilton, published in the Proceedings of the Second Meeting of the Mixed Commission on the Ionosphere in Brussels 1951 (3).

The contacts were rather surprising since the frequencies used exceeded the conventional MUFs for the circuits involved and path lengths were far in excess of that possible for a single hop mode via the ionosphere.

From the late 1950's ionospheric scientists took quite a deal of interest in this form of propagation and early efforts aimed at explaining the phenomenon attempted to correlate these unusual contacts with magnetic/ionospheric storms. (3), (4). However, only a few could be correlated with these storms and most contacts could not be explained in this fashion.

Observations made between 1950 and 1966 by a number of people of the characteristics and propagation modes of TEP (5-11), along with research into the equatorial ionosphere (11), brought to light a lot of very interesting information

about TEP. In addition to collecting Amateur observations, a number of experiments were set up involving HF and VHF scatter soundings, oblique incidence stepped frequency ionosondes, CW beacon observations, observations of TV and FM stations in Korea, Japan and Russia, and topside ionospheric sounding by satellites. These efforts led to a better understanding of the structure of the equatorial ionosphere and to suggestions regarding the various modes that support TEP (12).

However, all is not yet explained, and research is currently being carried out in Australia by the Department of Supply, the Ionospheric Prediction Service Division and the Physics Department of the James Cook University at Townsville. Of particular interest to the author is the night-time mode about which more will be said later.

The current research programme being carried out in the low latitude section of the IPSD includes the reception of beacon transmissions, examining the signal characteristics and corelating this information with other geophysical phenomena.

2. GENERAL CHARACTERISTICS OF VHF TEP SIGNALS

There appears to be two distinct types of TEP, distinguished by the times of peak occurrence, fading characteristics, path lengths, and the principal mode of propagation.

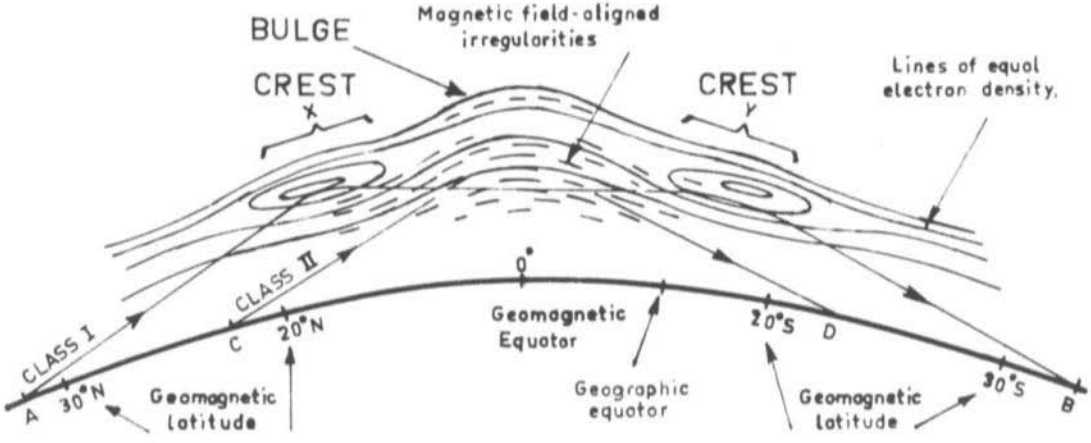

Fig. 1: The propagation modes of class I and class II TEP

One mode, designated Class I., exhibits the following characteristics:

a) A peak occurence around mid-to-late afternoon (1200 to 1900 local mean time, measured at the point where the path crosses the magnetic equator).

b) Normally strong, steady signals with a low fading rate and, more specifically, a small Doppler spread (around ± 2 to 4 Hz) (12)

c) Path lengths of 6,000 km. to 9,000 km. and sometimes longer.

The proposed propagation mode for Class I TEP is generally termed the "super-mode" or ^2F mode. As can be seen from Fig. 1, the ray, transmitted from A, "skips" from the crest in the equatorial ionosphere at X, across to the crest at Y and is refracted down to earth at B. These "crests" are a feature of the equatorial ionosphere about which more later.

The other mode, designated Class II., shows the following characteristics:
a) A peak occurrence around 2000 hours to 2300 hours local mean time.

b) High signal strengths but with deep, rapid fading (typical rates are 5 Hz. to 15 Hz.) accompanied by a Doppler spread much greater than for Class I. Generally the Doppler spread is in the order of ± 20 to 40 Hz. (i.e. ten times that for Class I.) (12).

c) Path lengths are usually shorter than for Class I., being around 3,000 km. to 6,000 km. Sometimes they are longer.

The propagation mode or mechanism for this class of TEP is not yet fully understood, but it is believed that irregularities (dense "clouds" of electrons having a certain specific shape) in the equatorial ionosphere, which are aligned with the earth's magnetic field, are responsible for "ducting" or efficiently "scattering" the signal such that the path geometry looks like that in Fig. 1 (from C to D) (12).

Additionally, Class II. will support much higher frequencies than Class I. and signals have been observed up to 102 MHz. This does not imply that 102 MHz. is the maximum frequency that Class II. TEP will support. It is just that nobody has reported an authentic case any higher in frequency.

Who will be the first to make Australia-Japan on 144 MHz via TEP? No upper limit has yet been proposed for Class II. TEP.

Class I TEP is sometimes called "afternoon-type TEP" and Class II is sometimes called "evening-type TEP" for obvious reasons.

Before discussing TEP in further detail, we should look at the equatorial ionosphere.

3. THE EQUATORIAL ANOMALY

The equatorial ionosphere does not have an even distribution of electron density. As can be seen from Fig. 1, the F-region iso-electronic contour lines (lines of equal electron density) show a depletion of electrons, together with a rise of the F-region height, above the magnetic equator. Roughly symmetric, north and south of the geomagnetic equator, are two "crests" that represent an increased electron density in the F-region. These crests are located between 10^o and 20^o (geomagnetic latitude) north and south of the geomagnetic equator (13). The location of these regions can be obtained from Figs. 2, 3 and 4 which are maps of the various continental zones with the geomagnetic latitude lines superimposed.

This region of the ionosphere (within approximately ± 20^o geomagnetic latitude) is generally referred to as the equatorial anomaly region despite the fact that it is a regular feature of the equatorial ionosphere.

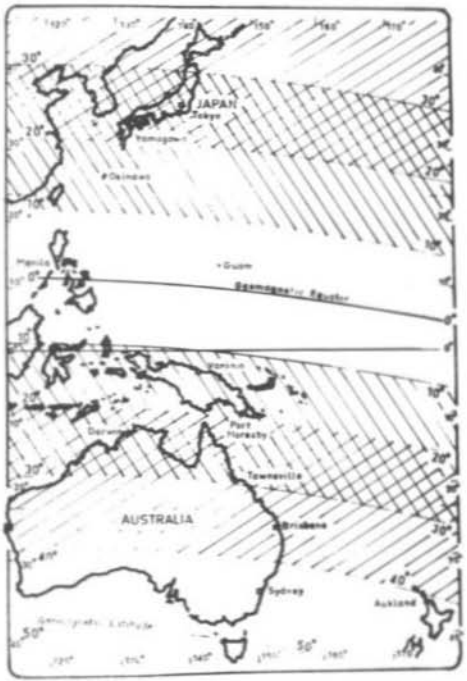

Fig. 2: Australian sector of the world showing terminal zones for class I TEP (20° to 40° geomagnetic latitude) and class II TEP (10° to 30° geomagnetic latitude)

Fig. 3: The American sector of the world showing terminal zones for class I TEP (20° to 40° geomagnetic latitude) and class II TEP (10° to 30° geomagnetic latitude)

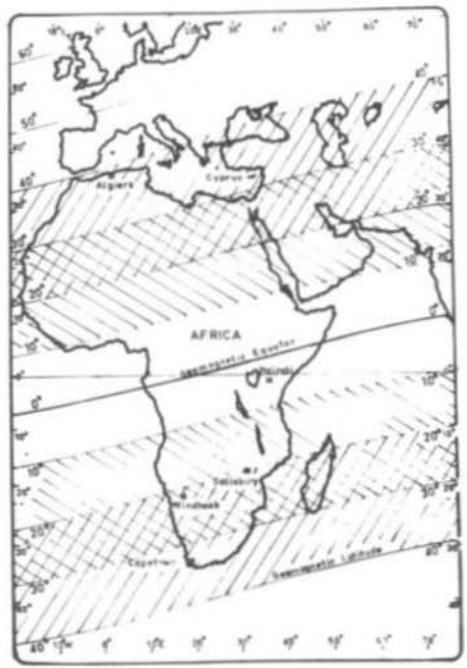

Fig. 4: The African-Mediterranean sector of the world showing terminal zones for class I TEP (20° to 40° geomagnetic latitude) and class II TEP (10° to 30° geomagnetic latitude)

If the electron density within the crests increases sufficiently it will be possible for a signal, incident upon one crest at a very small angle, to be refracted across the geomagnetic and geographic equators to the opposite crest and thence to earth as illustrated in Fig. 1.

4. VIRTUAL HEIGHT OF THE EQUATORIAL ANOMALY

The virtual reflection heights of signals in the anomaly zone varies between about 350 km and 550 km, (12), (13) giving path lengths in the order of 3,000 km. to 9,000 km (12) for signals propagated by the modes shown in Fig. 1.

5. DIURNAL VARIATION OF THE EQUATORIAL ANOMALY

In the Australasian sector of the world, the equatorial anomaly starts to develop between 0800 LMT and 1000 LMT, the crest moving away from the magnetic equator between 0700 LMT and 1500 LMT (13).

In the American sector, the development time of the equatorial anomaly is much more variable, but it is generally present after 1800 LMT. The build-up of the anomaly appears to occur between 1100 LMT and 1800 LMT. However, these statements must be tested further since they are based on very little data. Comparisons between the positions of the crests over the Australasian sector and the American sector at the same LMT show that they are further from the equator in the Australasian sector than they are in the American sector (13).

The behaviour of the anomaly in the African sector is similar to that in the Australasian sector.

When the sun sets on the base of the equatorial ionosphere (about 1.5 hours) later than ground sunset, i.e. 1930 hours LMT), the base of the layer generally rises and the equatorial anomaly begins to break up into large "blobs". This is not always so, the base of the layer may not necessarily rise and, on occasion, is found to fall or remain at the pre-sunset height. Sometimes the anomaly does not break up into distinct blobs and the electrons appear to diffuse over the magnetic equator. The ionosphere is generally like this during early morning and late evening (13). The detailed behaviour of the decay phase of the equatorial anomaly has not yet been fully established.

6. THE EQUATORIAL ANOMALY AND MAGNETIC ACTIVITY

On magnetically disturbed days the equatorial anomaly is not as well developed as it is on magnetically quiet days and it is known that, in the Australasian sector, the bulges are closer to the magnetic equator on disturbed days than on quiet days (13).

Recent research also indicates that, in the American sector, the anomaly develops earlier on very quiet days and in the late afternoon on disturbed days.

Insufficient work has been done in the Australasian sector to give a complete picture (which promises to be quite complex) of the influence of the level of magnetic activity on the equatorial anomaly.

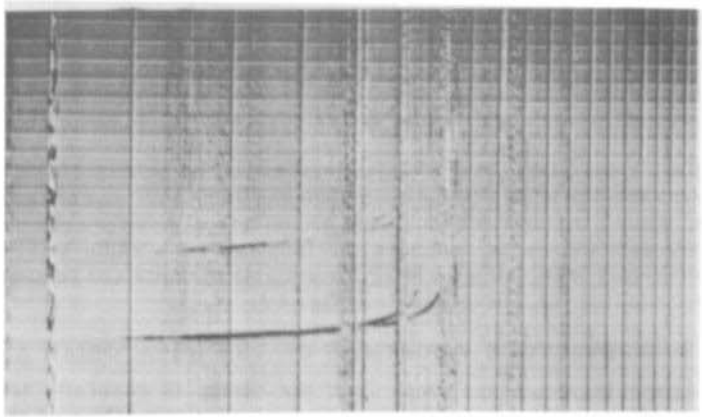

Fig. 5a: Vertical incidence ionogram from Cocos Island, 19.00 LMT, August 5 th, 1970, showing a typical F-layer trace without range spreading

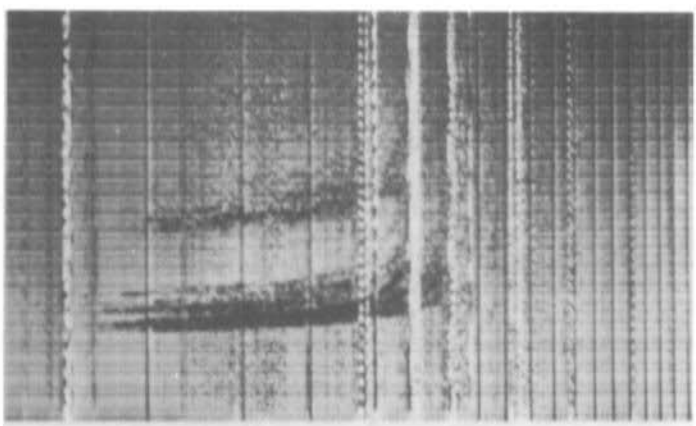

Fig. 5b: Vertical incidence ionogram from Cocos Island, 22.00 LMT, August 5 th, 1970, showing typical equatorial spread – For range spreading. Range spreading is caused by oblique incidence reflections from irregularities in the base of the F-layer

7. SEASONAL VARIATIONS OF THE EQUATORIAL ANOMALY

The crests lie very nearly symmetrically either side of the magnetic equator at equinox and asymmetrically at solstice. The electron densities of the bulges are greater at equinos than at solstice and this, combined with the anomaly symmetry at equinox, favours Class I TEP at the equinoxes. The separation and overall width of the crests varies seasonally also, being greatest at equinox.

"Tilts" in the base of the F-layer are known to be associated with the crests and are most pronounced between 1200 and 2000 LMT and at equinox (11). These tilts, which are departures of the iso-electron density contours from concentricity with the earth, enhance the tangency of a radio wave with the layer, consequently increasing the MUF for suitable circuits and improving the chances of propagation via a supermode (Fig. 1).

8. SUNSPOT CYCLE VARIATIONS OF THE EQUATORIAL ANOMALY

At sunspot maximum the break up of the crests is generally later than at sunspot minimum (11). This appears to be the major effect of the sunspot cycle on the equatorial anomaly.

The relative depletion of electrons over the geomagnetic equator is greater at sunspot maximum than at minimum. There is a consequent increase in the number of electrons in the crests at maximum and an increase in the presence of tilts, increasing the MUF.

The crests of the equatorial anomaly are present for fewer hours during sunspot minimum and their height, size, associated tilts and ionisation density decrease with decrease in sunspot number (11).

All these factors contribute to the observed dependence of Class I TEP on the sunspot number.

9. "SPREAD-F" OR "RANGE-SPREADING"

On some days irregularities start to appear in the base of the F-layer by 2000 hours LMT and cause what is termed "range-spreading" or "spread-F" on vertical incidence ionograms. An illustration is given in Fig. 5, comparing an "unspread" ionogram to one showing spread-F for different times on the same day at Cocos Island. The cause of these irregularities is not yet known. They are not necessarily associated with the decay phase of the equatorial anomaly. There appears to be a connection between spread-F and evening type TEP (14).

The duration of spread-F is quite variable, sometimes lasting for less than hour and at other times lasting until 0600 hours the next morning.

The occurrence of spread-F is more common on magnetically quiet days, in periods of sunspot maximum, and is more common in areas where the geomagnetic and geographic equators are widely separated (11). There appears to be no correlation between magnetic activity and spread-F at sunspot maximum.

The occurrence of spread-F favours the equinoxes, particularly in the Australasian sector (11), except at sunspot minimum where it favours the summer solstice. This effect is not so pronounced in the American sector.

Spread-F appears to be dependent on the post-sunset rise of the F-layer base which is most pronounced at sunspot maximum (11).

10. CLASS I TEP-CAUSES AND CHARACTERISTICS

It is now well established that Class I TEP depends on the equatorial anomaly. All the observed variations and characteristics of the equatorial anomaly influence Class I TEP in a predictable manner. However, what is the cause behind the cause? or, what causes these two crests that are a feature of the equatorial ionosphere?

10.1. THE FOUNTAIN EFFECT

During the day, electrons from the base of the F-layer move upwards, in the region of the magnetic dip equator (where the magnetic field lines are horizontal), under the combined influence of the earth's magnetic field and the electric field that exists between the E-layer and the F-layer. These electrons then diffuse along the magnetic field lines and accumulate at two places, either side of the magnetic equator, forming the crests of the equatorial anomaly (15). The effect is illustrated in Fig. 6.

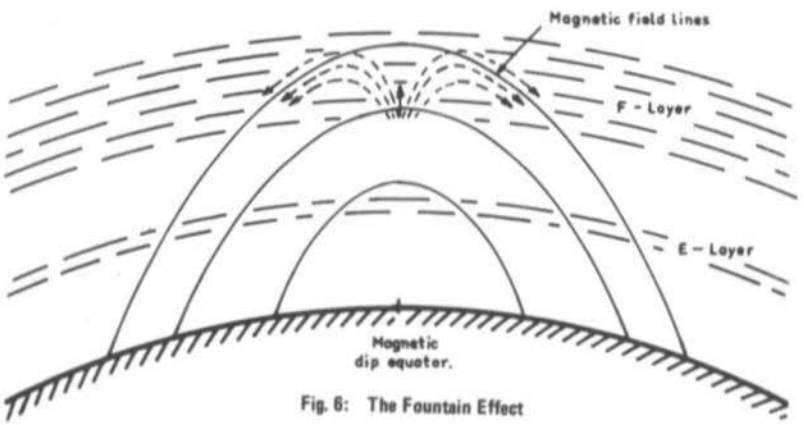

Fig. 6: The Fountain Effect

This explanation is, of necessity, simple and perhaps not entirely accurate, but should serve for the purpose of this article. For those who wish to know more, read reference (15).

The effect of the equatorial anomaly on foF2 (critical frequency of the ordinary ray at vertical incidence for the F2 layer) for the area either side of the geomagnetic equator is given in the inset of Fig. 7. As can be seen, foF2 reaches a peak where the crests are located and a trough over the magnetic equator. This partly accounts for the high MUFs observed when supermode propagation is used.

11. DETAILED CHARACTERISTICS

The characteristics of Class I TEP will now be discussed in detail with reference to its dependence on the equatorial anomaly. The reader can refer back to particular paragraphs in the discussion of the equatorial anomaly if necessary to elucidate the dependence of various characteristics on the associated characteristics of the equatorial anomaly.

11.1. OCCURRENCE TIMES

There is a peak occurrence of Class I TEP between 1200 and 1900 LMT for all sectors. Individual circuits will have slightly different peak occurrence times somewhere within these limits. The peak occurrence times coincide with the stable phase of the equatorial anomaly which is generally well developed after 1100 LMT and begins to decay around 1900 LMT. Occasionally it remains stable after this time, particularly at equinox at sunspot maximum (11) and observations bear this out, signals remaining stable for several hours after 1900 LMT before experiencing the flutter fading of Class II TEP (12).

Paths that are normal (or nearly so) to the geomagnetic equator and symmetrically located either side are favoured, experiencing earlier start times, longer durations and a greater number of occurrences - especially at sunspot minimum.

Australia and Asia-Japan are ideally situated in this regard as are Central/South Africa and North Africa/Mediterranean. The Americas are not so well off except for circuits involving Venezuela, Guyana, Surinam, etc., and Chile/Argentina. See the maps in Figs. 2, 3 and 4.

TEP can occur at any time of the night or day, but it is most infrequent between 0400 and 0800 LMT (11) for either Class I or Class II TEP.

Occurrence times are generally dependent on: -

a) Suitable path geometry, including tilts which allow supermode propagation.

b) Build up of sufficient ionisation density in the crests of the equatorial anomaly such that foF2 of each crest is sufficiently high to increase the MUF above that normally expected.

c) Sunspot number (b) is obviously dependent on sunspot number, but this is not the only factor involved. This dependence is not as great as one would imagine and is much less than for Class II.

d) Season.

11.2. PATH CHARACTERISTICS

As Class I TEP is propagated via a supermode (Fig. 1) the path geometry can be determined for the maximum and minimum range possible for the observed parameters of the bulges of the equatorial anomaly. The parameters affecting the path geometry are the height and location of the virtual reflection points, foF2 for these points and incidence angles to those points. Knowing these, it becomes possible to predict the maximum and minimum ranges. These work out to be between 5,000 and 9,000 km (12). This was calculated assuming that the path and equatorial anomaly were symmetrical about the geomagnetic equator.

Oblique paths and asymmetrical paths will encounter different conditions about which more will be said later.

The best paths are those which are located symmetrically about and normal (or nearly so) to the geomagnetic equator and the terminals of which lie in areas between 20° and 40° geomagnetic latitude north and south of the geomagnetic equator. These areas are marked in Figs. 2, 3 and 4 (cross hatched to the right). These paths tend to experience Class I TEP more often than oblique or asymmetrical paths.

Very long paths (greater than 10,000 km.) are always oblique and some other form of propagation appears necessary to assist the signal in being favourably incident on the bulges of the equatorial anomaly. Sporadic E (Es) is the most likely cause but this has yet to be confirmed. An observation by Roger Hord, VK 2 ZRH (private communication) appears to support this. On 8th November, 1970, he reported hearing WB 6 KAP on 50 MHz. from 1310 to 1435 EAST. At the same time he reported sporadic E signals from New Zealand. Now WB 6 KAP is located in California some 12,000 km. from Sydney. For this signal to have been refracted across the equator via a supermode, it must have struck the southern crest of the equatorial anomaly somewhere above Western Samoa which is some 4,500 km from Sydney. A ray, leaving the earth tangentially would strike the F-layer some 2,000 km away at the most. Thus some other form of propagation was necessary for the signal to reach Sydney. It works out that it is possible for sporadic E, located over the Tasman Sea east of Australia, to refract the signal sufficiently for it to arrive at the equatorial anomaly over Western Samoa.

Southern California is located sufficiently close to the geomagnetic equator for a ray to strike the equatorial anomaly at a favourable angle.

A ^3F mode has been suggested (11), but as yet is unconfirmed. Its likelihood is rare.

TEP over paths which are fairly oblique to the geomagnetic equator (65° or less) tend to be reasonably long (greater than 8,000 km.), rare, short lived and tend to occur mainly some weeks after the equinoxes. Many of them are asymmetrically situated with regard to the geomagnetic equator, but this bias is probably due to observer station distribution. Very long range TEP is generally observed one to two years after a sunspot maximum and rarely, if ever, during the sunspot minimum.

11.3. RAY TRACING

If a series of rays from a transmitter in one hemisphere is traced, using computer simulation through a model of the equatorial ionosphere, it is found that much of the low angle radiation travels via the supermode of propagation and experiences a large degree of focussing at the receiver.

In Fig. 7, a computer printout is shown illustrating this ray-focussing effect. The inset shows the variation of foF2 with geomagnetic latitude assumed for the particular circuit. The printout is reproduced here with the kind permission of Mr. B.C. Gibson-Wilde, of the James Cook University of North Queensland.

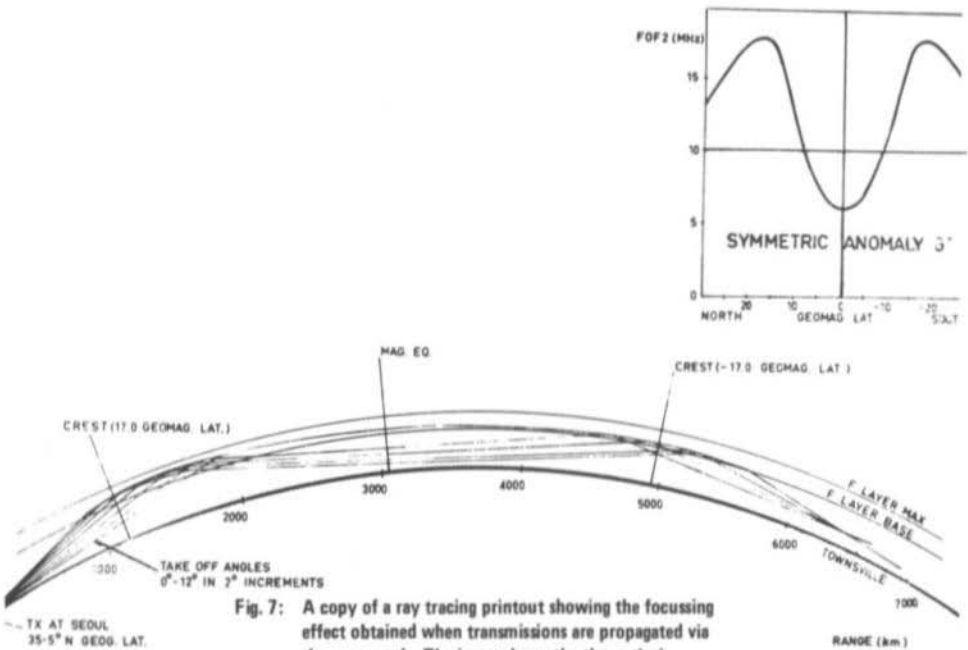

Fig. 7: A copy of a ray tracing printout showing the focussing effect obtained when transmissions are propagated via the supermode. The insert shows the theoretical symmetric anomaly assumed in the ray tracing program that produced the printout

Ray focussing is a very important characteristic of Class I TEP as it provides the strong signals and "area selectivity" (signals being heard in one narrowly defined area and not in others) that is often noticed as being associated with afternoon type TEP (10) (also reported by D. Tanner, VK 8 AU, private communication).

Many observers have noted that, from their location, TEP signals are observed first from the most eastern area and thence move west - following the sun. For example, Amateurs in the Eastern States of Australia first hear Amateurs in the eastern regions of Japan. The eastern stations gradually disappear and are followed by stations in central Japan, then western Japan, then Korea. Japanese Amateurs first hear stations in the eastern States (Qld., N.S.W., Vic.) and then stations in central regions of Australia (N.T., S.A.) followed by stations in Western Australia.

Referring back to the diurnal variations in the equatorial anomaly, you will notice that the build-up of ionisation in the crests is time dependent and hence the critical frequency is time dependent. Thus the region of maximum ionisation will follow the sun and will have a westward motion. Consequently contacts between Australia and Japan would be expected to commence first in the east and move westward.

11.4. SEASONAL CHARACTERISTICS

There is a maximum number of occurrences around the equinoxes for all sectors of the world. This is due to the more favourable conditions that exist in the equatorial anomaly at the equinoxes. Reference to the seasonal variations in the equatorial anomaly will show that the important parameters satisfy the best conditions for Class I TEP at the equinoxes. The attitude of the earth with respect to the sun and the ecliptic plane is obviously the major controlling factor on the symmetry of the equatorial anomaly at equinox.

There is always a greater number of occurrences of Class I TEP near the sunspot maximum than during the minimum. It is well known that sunspot number affects the MUF of the F-layer and foF2 for the crests of the equatorial anomaly follow a similar pattern.

However, the greatest number of occurrences of Class I TEP lags behind the sunspot maximum by one to two years. The reason for this is, as yet, unknown (11).

Contacts can be had almost daily around the equinoxes with Class I TEP as was evidenced by the openings reported in "Amateur Radio" (16) and "QST" during 1970 and 1971 as well as earlier in "QST" (1), (2). Similar results are recorded by oblique ionosondes operating on transequatorial circuits between Okinawa and St. Kilda (S.A.) and Okinawa and Townsville (Qld.).

11.5. SIGNAL CHARACTERISTICS

Apart from the frequencies involved, the most extraordinary characteristics of Class I TEP signals are their strength and steadiness (absence of fade). Signal strength can sometimes approach free space values (12) and the fading rate is normally quite low and not very deep (1-3), (10-12). This is explained by the fact that rays strike the tilts associated with the crests of the equatorial anomaly very near to tangency and are efficiently refracted; this combined with ray focussing, and the same absorption for a one-hop path, leads to very little signal loss (7), (8), (10) and (11).

Many Amateurs report good results running only medium to low power (under 20 watts) and small antennas (16) (also in private communications).

The low fading rate is also associated with a low Doppler shift - generally around $\pm$ 2 to 4 Hz (12). If a power spectral density graph (signal power level versus Doppler shift) is examined for Class I TEP signals, it is observed that most of the Doppler shift is less than $\pm$ 2 Hz with another, smaller, peak at $\pm$ 4 Hz (12).

The peak MUF for Class I TEP appears to be around 60 MHz (12) which places the 6 metre Amateur band in a very fortunate position.

The frequencies involved in Class I TEP will always be above the predicted MUF, for the path involved, by a considerable factor. So you can see that Class I TEP affects the HF region as well as the lower VHF region. Contacts on the HF bands via Class I TEP have been reported (12), but are not often recognised by Amateurs.

The MUF for oblique paths is generally lower, owing to unfavourable "look" angles on the equatorial anomaly, and consequently the MUF for these paths exceeds 50 MHz less often than for paths which are more nearly normal to the magnetic equator (7), (11) and (12).

Although Class I TEP provides fairly stable signals, wideband systems will suffer distortion due to multipath effects (see Fig. 7). Voice transmissions will not appreciably suffer, especially FM, but television picture signals will be of very poor quality (12).

It must be understood that Class I TEP is not a "normal" F2 mode of propagation as many VHF Amateurs seem to think, but it is certainly not "anomalous" within the definition of the word. The MUF of the F-layer for ^1F or ^2F modes in general rarely exceeds 50 MHz so that Class I. TEP cannot be classed as "normal" F2 skip on these grounds alone. Secondly, Class I TEP travels via a two-hop ionospheric mode without intermediate ground reflection. This supermode or ^2F-mode is sometimes referred to as "chordal-hop" propagation.

- to be continued -

CORRECTIONS AND IMPROVEMENTS TO
THE DC 6 HL SSB TRANSCEIVER

1. PC-BOARD DC 6 HL 001

Due to a film-retouching error the interconnection of the two short conductor lanes between the ring modulator (D 120 to D 123) and inductance L 111/capacitor C 168 (270 p) no longer exists. A bridge should be made at this point.

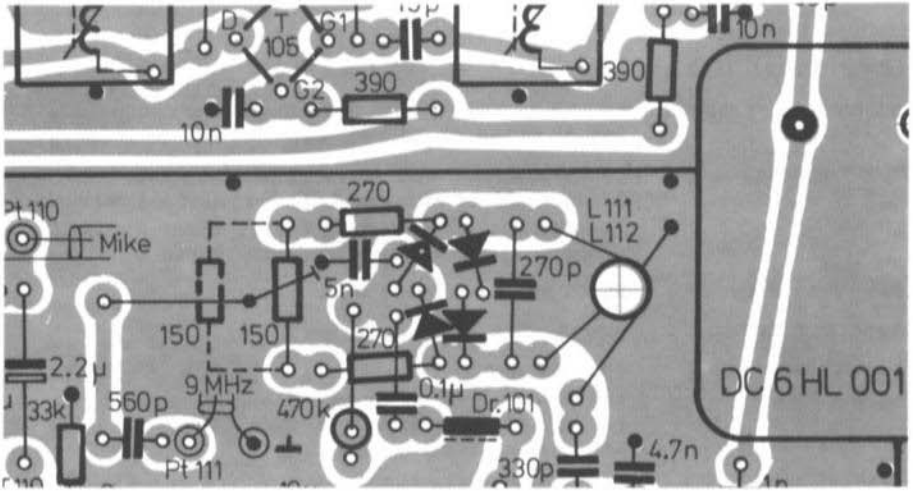

2. LOCAL OSCILLATOR MODULE DC 6 HL 003

Difficulties have been encountered by some constructors in obtaining a sufficient output voltage at 135-137 MHz. A discussion with the author at the Weinheim VHF meeting suggested the following possible cause of this:

The number of turns for L 312 to L 317 was reduced from the author's original 5 turns to 4 in the description and a VHF core was used instead of the RF-core used by the author in his prototype. This has caused the coupling to be too loose. It is therefore recommended that the original spaced 5 turns used in the author's prototype with RF core (red marking) be used. Since this core will not be inserted so far into the inductance, the strayfields of the inductances will be greater which will increase the coupling of the bandpass filters.

OSCAR 6
from AMSAT NEWSLETTER September 1972

Now that OSCAR 6 has been successfully launched it is thought that a few technical details will be of interest.

1. ORBITAL DATA

The following orbital data is valid for the ITOS-D and OSCAR 6 satellites:

Altitude: 1460 km
Period: 115.1, sun-synchronous
Inclination: 101°
Orbits per day: 12.5, i.e. passes repeat on the same time on a two-day cycle
Pass time: Approx. 9.00 (N-S) and 21.00 (S-N) local time regardless of location.
Longitude increment: 28.81° per orbit

2. TECHNICAL DATA

Input frequency range:	145.90 to 146.00 MHz for normal operation 145.83 to 146.07 MHz for extended passband operation
Output frequency range:	29.45 to 29.55 MHz for normal operation 29.38 to 29.62 MHz for extended passband operation Passband is non-inverting (i.e., upper sideband remains upper sideband and vice versa).
Beacon frequency:	29.45 MHz and 435.1 MHz
Beacon modulation:	Morse code (A-1 emission)
Repeater bandwidth:	100 kHz flat 120 kHz at 3-dB down points 150 kHz at 6-dB down points 240 kHz at 10-dB down points
Operating modes:	SSB and CW are recommended AM, RTTY and SSTV can also be used but with less efficiency. FM is not recommended
Repeater power output:	1 to 1.3 watts CW into a half wave dipole
Input sensitivity:	Approximately -100 dBm (2 microvolts/m) for full output
Ground power required:	80 to 100 watts of effective radiated power produces full output from the repeater at a maximum range of 2,000 miles. (An 8 to 10 watt transmitter and 10 dB of antenna gain, or 80 watt transmitter and omnidirectional antenna should be adequate).
Intermodulation:	20 dB down
AGC:	Up to 26 dB gain reduction 0.1 second attack time 2.2 second release time designed for highest efficiency with SSB

Ground receiver required: Better than 1/2 microvolt/m sensitivity for 10 dB (S + N)/N on 10 meters should be adequate. Dipole antenna can be used, but beam is preferable.

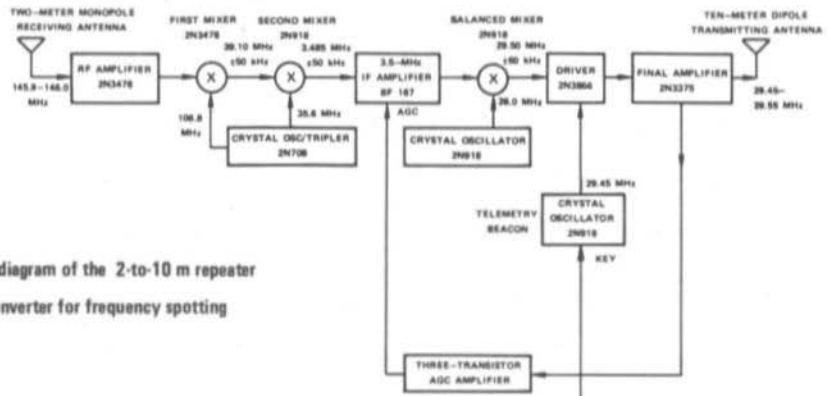

Fig. 1: Block diagram of the 2-to-10 m repeater

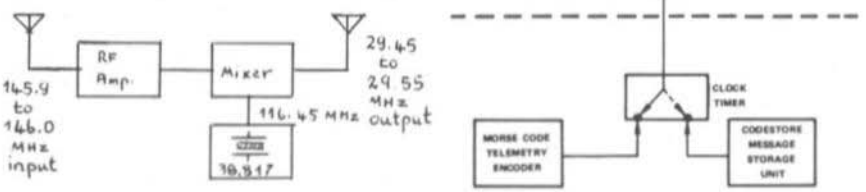

Fig. 2: 2 m converter for frequency spotting

3. INSTRUCTIONS FOR OPERATION VIA OSCAR 6

The repeater is designed for linear operation and is capable of handling most forms of narrowband modulation, SSB, CW, AM, FM, RTTY and SSTV. SSB and CW are recommended primary modes of operation and make most efficient use of the repeater because a number of users can operate simultaneously, each taking different proportions of the repeater's power capability at a particular instant of time. Therefore, a higher average power level is available to each user since not all CW users are key-down at any given instant, nor are all sideband stations talking up to full power

To facilitate the most efficient operation of the repeater, all users are strongly urged to continuously monitor their own downlink signals. This is an operation technique previously rarely available to amateurs, but which enables each user to hear his own signal from the satellite as others hear it. It requires simply that a separate receiver and antenna be available for receiving one's own downlink signal on ten meters, while transmitting simultaneously on the two-meter uplink band. Such operation makes possible perfect break-in QSO's and round-tables, particularly on SSB, permitting full duplex operation. Unlike other forms of amateur communications, satellite communications with downlink self-monitoring permits each user to observe how the DX hears his signal, and he can then adjust his power and frequency to compensate for the satellite's distance and Doppler frequency shift. This is most readily done by observing the satelli-

te's beacon signal level on 29.45 MHz and adjusting the power of the ground transmitter so that the repeated signal from the satellite appears to be the same level, either as read on an S-meter or as determined aurally. If the transmitter is VFO controlled, its frequency should be constantly adjusted by the operator while transmitting to keep the apparent downlink frequency constant in the presence of changing Doppler shift, which can be as much as $\pm$4.5 kHz for an overhead pass.

Spotting one's own downlink carrier is not always easy through the satellite repeater, and it is quite difficult to zero beat another station without careful dial calibration. One excellent method of getting a "frequency spotter" is to obtain a two-meter converter having either a 10 or 20 meter output and use it as a satellite repeater simulator in the shack. If the converter uses a 38.666 or 43.333 MHz crystal, replacing it with a 38.817 MHz crystal will convert locally generated two-meter signals in the 145.9 to 146.0 MHz uplink band to the correct frequency in the 29.45 to 29.55 MHz downlink band, so that spotting and zero beating can be accomplished without the signals leaving the shack. Figure 2 shows a block diagram of a repeater spotter for the shack. Because of Doppler shifts up to $\pm$4.5 kHz which will occur when using the actual satellite repeater, the spotter's frequency will be off by the amount of the Doppler shift. This can easily be corrected for by setting the transmitter frequency several kHz higher than the spotted frequency near the beginning of a pass, or several kHz lower than the spotted frequency near the end of a pass.

OPERATING PROCEDURE

The procedure recommended for operating with the OSCAR two-to-ten meter repeater is as follows:

1) When the satellite comes within range, begin listening for the Morse code beacon signal on 29.45 MHz. Be sure to note the signal strength of the beacon signal. Since the beacon is A-1 emission, use your BFO to receive it.

2) Once you have located the beacon on 29.45 MHz, tune up the band and begin looking for signals from the repeater in the 29.45 to 29.55 MHz range.

3) When you are ready to transmit, choose a frequency within the 145.90 to 146.00 MHz uplink band and send a test signal, preferably a string of dots, on this frequency (f_2). Listen for your own signal retransmitted from the satellite on the corresponding ten meter frequency (f_{10}), found from the formula:

$$f_{10} = f_2 - 116.45 \text{ MHz} \pm f_{Doppler}$$

where $f_{Doppler}$ = +4.5 kHz near the beginning of an overhead pass
= 0 kHz at the middle of the pass
= -4.5 kHz near the end of an overhead pass.

For example, a signal transmitted on 145.92 MHz will be retransmitted on 29.47 MHz $\pm$ Doppler. This is where you should listen for your signal. If you can hear your own signal, you can be sure that others can hear your signal as well.

4) Adjust your transmitter power so that on SSB voice peaks or with a slow string of dots the repeated signal is approximately equal to the beacon signal level. This will assure that you take the correct share of the repeater power without overloading the repeater and running down the satellite's battery unnecessarily. Keep in mind that the power will be divided among all stations in the passband. An overly strong station will prevent other amateurs from simultaneously using the repeater if he does not reduce his power. He will also reduce the overall repeater gain, through AGC action, so that he will not be able to hear weaker stations who may be trying to call him. If you do not have a convenient method for directly controlling your power output, an alternative technique is to aim your antenna away from the satellite.

If you intend to operate with high power or use a large antenna array such that the transmitted output multiplied by the antenna gain is above 80 to 100 watts effective radiated power, then it is suggested that you operate slightly off from the regular passband of 145.90 to 146.00 MHz. The repeater has an "extended passband" feature in its design, that is the -10 dB response is $\pm$120 kHz from the center frequency (the passband is 240 kHz wide at the 10-dB down points). Therefore, if higher power stations will transmit between 145.83 and 145.89 MHz or from 146.01 to 146.07 MHz, their signals will be compensated for by the roll-off of the repeater response, and they will not take more than the correct portion of the repeater power. One benefit for doing this is simply a reduction in QRM, since only high power stations can operate through the repeater on these extended frequency segments. Low power stations cannot easily overcome the additional attenuation of the passband roll-off and should operate in the normal repeater passband of 145.90 to 146.00 MHz.

AN INTEGRATED RECEIVER SYSTEM FOR AM, FM, SSB and CW

by H. J. Franke, DK 1 PN

The British company Plessey offers a number of integrated circuits which allow receivers and transmitters for the various frequency ranges to be completely, or partly, integrated. One will especially notice the extremely low number of external components that are required in addition to the inavoidable resonant circuits. This means that it is possible to construct small, reliable and extremely effective equipment which is not only suitable for fixed station use but especially for mobile and portable operation.

1. RF AND IF AMPLIFIERS SL 610 C, SL 611 C, SL 612 C

These integrated circuits are wideband amplifiers that are suitable for use with an operating voltage in the range of 5 to 10 V. The given specifications are valid for an operating voltage of 6 V, which can also be classed as the recommended operating voltage. The gain can be varied in a range of at least 40 dB (typ. 50 dB) by connection of an external, variable DC-voltage; with the SL 612 C the values are a minimum of 60 dB (typ. 70 dB). Types SL 610 C and SL 611 C can be used up to a frequency in the order of 100 MHz; the SL 612 C is of higher impedance and possesses a 3 dB frequency limit of only 15 MHz. However, it offers a higher gain, lower noise figure and lower current drain. The most important specifications of the given integrated circuits are listed in the following table. An extremely good cross-modulation rejection, which is extremely important for receiver applications, can be obtained by external feedback.

The values given in the following table are valid, when not otherwise mentioned, for an ambient temperature of 25 °C, an operating voltage of 6 V and without control voltage. Connection 5 and 6 are connected together (Fig. 1).

Measurement	Type	min.	typ.	max.	Notes
Voltage amplification	SL 610 C	18 dB	20 dB	22 dB	30 MHz
	SL 611 C	24 dB	26 dB	28 dB	30 MHz source 2 kΩ; load 5 kΩ/8 pF
	SL 612 C	32 dB	34 dB	36 dB	1.8 MHz
3 dB limit frequency	SL 610 C	85 MHz	140 MHz	-	
	SL 611 C	50 MHz	100 MHz	-	source: 25 Ω; load: no-load
	SL 612 C	10 MHz	15 MHz	-	
Max. input voltage for 1% cross-modulation, uncontrolled:	SL 610 C	-	100 mV	-	10 MHz, load greater than 150 Ω.
	SL 611 C	-	50 mV	-	
	SL 612 C	-	20 mV	-	1.75 MHz; load greater than 1.2 Ω.
controlled:	all three	-	250 mV	-	10 MHz, or 1.75 MHz for SL 612 C.
Control range	SL 610 C	40 dB	50 dB	-	
	SL 611 C	40 dB	50 dB	-	
	SL 612 C	60 dB	70 dB	-	
Current drain of the AGC input	SL 610 C	-	0.15 mA	0.6 mA	
	SL 611 C	-	0.15 mA	0.6 mA	at a control voltage of 5.1 V
	SL 612 C	-	0.15 mA	0.3 mA	
Quiescent current drain	SL 610 C	-	15 mA	18 mA	
	SL 611 C	-	15 mA	18 mA	outputs under no-load
	SL 612 C	-	3.3 mA	4.3 mA	

The maximum permissible operating voltage of 12 V should not be exceeded under any circumstances.

2. AGC VOLTAGE GENERATORS SL 620 C and SL 621 C

Both of these integrated circuits generate a control voltage from the AF signal. The SL 620 C is dimensioned so that it generates a control voltage for audio amplifiers with dynamic compression, whereas the SL 621 C has especially been developed for SSB receivers. The control voltage possesses a certain delay time, which means that the circuit will not provide the full sensitivity during the speech pulses, but the return to the higher gain commences after a certain delay. This means that background noise or interference is not heard immediately. The integrated circuit SL 621 C is especially suitable for use with the RF and IF amplifiers SL 610 C, SL 611 C and SL 612 C, whereas the SL 620 C has been especially designed for use in conjunction with the AF amplifier SL 630 C.

These two integrated circuits are also designed for a nominal operating voltage of 6 V, where a current drain of max. 4.1 mA is present. A special feature of these two circuits should be pointed out: Each of these integrated circuits consists internally of two separate systems for generation of the control voltage that each have different time constants. It is always the greater of these two voltages which is provided as output signal. In this manner, it is ensured that short-term interference is quickly controlled without having to shift the basic level of the control voltage that originates from the required signal. Otherwise, the interference would cause a blocking effect, or reduction of reception for a certain period.

3. THE AF-AMPLIFIER SL 630 C

The AF-amplifier SL 630 C is especially suitable for use in SSB receivers and transmitters, however, it is also suitable for use in equipment for other modes. This integrated circuit can provide an output power of over 200 mW which is sufficient for driving small loudspeakers and more than sufficient for earphones. The voltage amplification is in the order of 38 to 49 dB according to tolerance, and circuit. The input can be driven either floating or grounded with the aid of a coupling capacitor according to the application. A dynamic microphone can be directly connected without coupling or decoupling capacitor. It is only necessary for the screening of the microphone cable to be grounded.

An external capacitor can be added at a point having a defined impedance in order to determine the upper limit frequency. At a nominal operating voltage of 6 V, the quiescent current drain is max. 5 mA. Under full drive conditions, an output power of 100 mW is provided into a load of 16 Ω at low distortion. At 12 V, an output power of 200 mW can be provided into a load impedance of 40 Ω. The highest permissible operating voltage is 15 V. The gain can be varied by provision of a variable DC voltage at the control voltage input. Since no AF voltage is fed to the potentiometer the danger of introducing RF and hum voltages is considerably reduced. After exceeding a threshold voltage of approximately 0.8 V, the gain will be reduced logarithmically on increasing the control voltage; this means that the use of a linear potentiometer will result in a psophometric, logarithmic volume adjustment. The gain can also be controlled automatically with the aid of the SL 620 C control voltage generator which means that a dynamic compression can be obtained in a very simple manner.

4. BALANCED MODULATORS SL 640 C and SL 641 C

The operation of these integrated circuits is based on that of a ring mixer. They allow balanced mixers to be constructed that exhibit good carrier suppression up to a maximum frequency in the order of 70 MHz. The built-in phase reversal stages mean that no external balancing transformer is required. The carrier suppression without external circuitry is in the order of 40 dB and can be increased to 60 dB with the aid of simple alignment measures. At full drive (required signal approximately 50 mV so that only a very low degree of preamplification is required), the intermodulation products will be at least 30 dB (typ. 45 dB) down on the required signal.

The integrated circuit SL 640 C, which has been designed for transmit applications, is provided with a built-in load resistor with subsequent emitter follower and possesses a low impedance output. The collectors of the mixer transistors are accessible with the SL 641 C so that an IF resonant circuit can be connected. In addition to this, the SL 641 C possesses a lower noise figure and somewhat lower current drain than the SL 640 C. At 6 V, the current drain is in the order of 10 mA (max. 13 mA); with the SL 640 C, the current drain is 12 mA (max. 16 mA). The maximum permissible operating voltage is 9 V.

5. A 9 MHz RECEIVE SYSTEM FOR AM, FM, SSB and CW

The application of these integrated circuits in a 9 MHz receive system into which converters for the various VHF and UHF bands can be fed is now to be given as an example. This single conversion superhet principle with a crystal filter directly following the mixer stage guarantees the best possible large-signal behaviour (3). Figure 1 shows a preliminary block diagram of the receiver which comprises 6 modules that are accommodated in TEKO cases of sizes 1A, 2A or 3A.

The VHF portion DJ 9 ZR 006 (1) is suitable for converting the 144 - 146 MHz signal to 9 MHz in conjunction with the DJ 5 HD 001 synthesis VFO for 135 - 137 MHz (2).

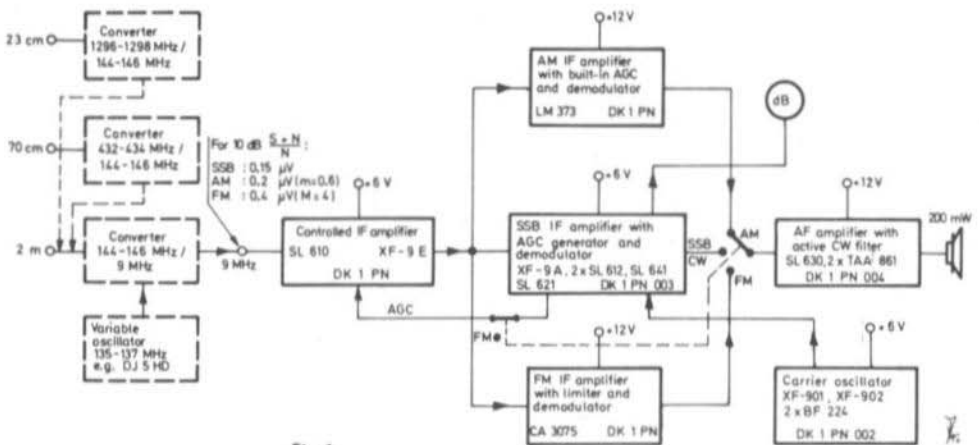

Fig. 1

The 9 MHz output signal from the converter is fed to the first DK 1 PN module incorporating the FM crystal filter XF-9 E and the controlled amplifier SL 610. After the insertion loss of the filter has been deducted, the gain of this module amounts to max. 20 dB. The ultimate selectivity is determined by the crystal filter which means that a crystal filter XF-9 A can be used in module DK 1 PN 003 for reception of SSB signals.

Three different IF amplifiers are connected in parallel to the input module. All of the IF strips remain connected and are not switched. The SSB module DK 1 PN 003 has been built up according to the manufacturer's recommendations. The AM IF amplifier DK 1 PN 006 is equipped with the very complex integrated circuit LM 373 manufactured by National Semiconductor. This integrated circuit comprises a controlled amplifier, a control voltage generator and demodulator. The FM IF strip is also only equipped with one integrated circuit, a CA 3075 manufactured by RCA. It is equipped with a limiter and coincidence demodulator. At present, tests are being carried out to use the newer CA 3089 E in the FM IF portion.

The AF amplifier module DK 1 PN 004 is switched to the required IF strip. It is equipped with the AF amplifier SL 630 manufactured ba Plessey and two operational amplifiers TAA 861 manufactured by Siemens, which form an active telegraphy bandpass filter. The AF amplifier SL 630 is connected so that only the voice frequency range is passed. This results in a considerable improvement of the receiver's sensitivity (signal-to-noise ratio).

The carrier oscillator module DK 1 PN 002 possesses a separate oscillator for each crystal. Each oscillator has been dimensioned for the lowest possible distortion. In the SSB and CW mode, the oscillator voltage is fed to the integrated balanced mixer SL 641 in module DK 1 PN 003. The sensitivity values given in the block diagram are valid for 10 dB signal + noise/noise measured at the loudspeaker output of the AF amplifier. This sensitivity can be obtained with a converter gain of approximately 20 dB.

The mentioned modules are to be described in the following editions of VHF COMMUNICATIONS.

6. REFERENCES

(1) K. P. Timmann: A 145 MHz/9 MHz Receive Converter Using Printed Inductances
VHF COMMUNICATIONS 1 (1969), Edition 3, Pages 129-135

(2) G. Bergmann and M. Streibel: A Synthesis VFO for 144 - 146 MHz or 135 - 137 MHz
VHF COMMUNICATIONS 3 (1971), Edition 1, Pages 44-45

(3) D. E. Schmitzer: A Modern Concept for Portable 2 metre Receivers
VHF COMMUNICATIONS 1 (1969), Edition 2, Pages 115-122

DIMENSIONING OF MICROSTRIPLINE CIRCUITS
Part 2

by W. Schumacher, DJ 9 XN

6. EXAMPLES OF THE COMPUTATION OF LINE CIRCUITS USING THE SMITH DIAGRAM

The following values are valid for all printed circuit boards: $\varepsilon_r = 5$, thickness $h = 1.4$ mm. The diagrams given in (4) form the basis for the dimensioning of the striplines.

6.1. DEVELOPMENT OF A CAPACITIVELY SHORTENED λ/4 RESONATOR

The dimensioning is made according to Figure 3 ignoring the circuit losses. The shortening capacity C (5 pF), the impedance Z_L (60 Ω) and the resonant frequency f_R (434 MHz) are known. Required is the mechanical length of the stripline circuit. The conductor lane width for 60 Ω amounts to: $w/h = 1.25$; $w \approx 1.9$ mm.

$$\lambda_{st}/\lambda_o = 0.575, \quad \lambda_o = 69.1 \text{ cm}, \quad \lambda_{st} = 39.8 \text{ cm};$$

$$B = \omega C = 2\pi \times 434 \times 10^6 \times 1/S \times 5 \times 10^{-12} \, A_s/V = 13.9 \text{ mS}$$

Standardized susceptance $b = B \times Z_L = 0.835$. The transformation steps in the Y-type Smith diagram are as follows (see Fig. 21). The commencement is the no-load point NL (ideal parallel resonance). The magnitude b is connected in parallel which corresponds to a shift along the curve $|r| = 1$ in the direction of the short circuit point from $b = 0$ to $b = 0.835$. From there, the line will cause a further transformation along the same curve at the angle $l/\lambda = 0.139$ up to the short circuit point. This means that the length is also known:

$$l = 0.139 \times 39.8 \text{ cm} = 5.532 \text{ cm} \quad (\lambda = \lambda_{st})$$

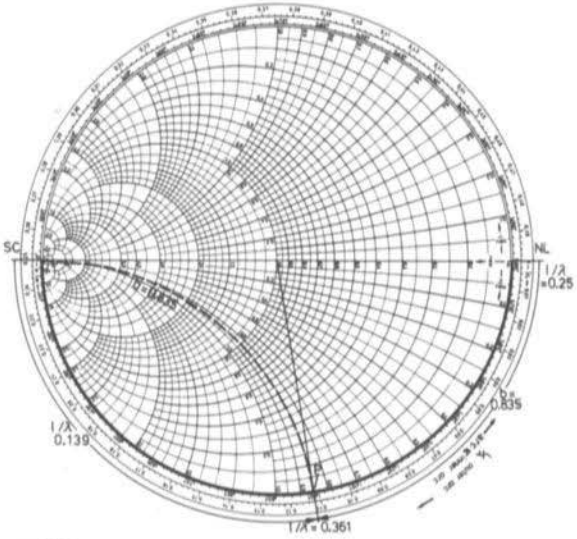

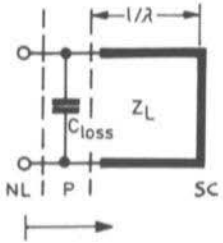

Fig. 21: Capacitively shortened λ/4-circuit in a Smith diagram

6.2. COMPUTATION OF A STRIPLINE FILTER FOR THE 24 cm BAND

The principle is given in Figure 22: A line of different impedance (Z_{L2}) having exactly the length $\lambda/2$ at a prescribed frequency f_R is placed into line Z_{L1}. At this frequency, an exact 1 : 1 transformation of the impedance in plane A to that of plane D will take place. Since the impedance A corresponds to the impedance Z_{L1}, Z_D will be equal to Z_{L1} at λ_R (the line at the output can be of any length since it is terminated with Z_{L1}). A certain reactive component will be present at all other frequencies that will cause a reflection of the energy. This arrangement therefore has the effect of a filter.

In order to be able to use available connectors, Z_{L1} has been selected to be 50 Ω. The higher the impedance variation during the transformation process, the steeper will be the skirts of the bandpass characteristic. Since the highest impedance with $\varepsilon_r = 5$ amounts to $Z_L = 130\ \Omega$ the following will be valid:

$$tr^2 = / Z_{L2} / / / Z_{L1} / = 2.6$$

If, however, the transformation is made to a lower impedance, for instance to $Z_{L2} = 10\ \Omega$, a greater impedance jump will be possible since the conductor lanes will be wider. The transformation path will be easily found in the Smith diagram under resonant conditions (Figures 22 and 23). According to (4), the following values result:

$f_R = 1300$ MHz, $\lambda_R = 23$ cm, $\varepsilon_r = 5$, $h = 1.4$ mm
$Z_{L1} = 50\ \Omega$, $w/h = 1.7$; $w_1 = 2.4$ mm, length as required,
$Z_{L2} = 10\ \Omega$, $w/h \approx 10$; $w_2 = 14$ mm, $\lambda_{st}/\lambda_o = 0.53$; $l = \lambda_{st}/2 = 6.1$ cm

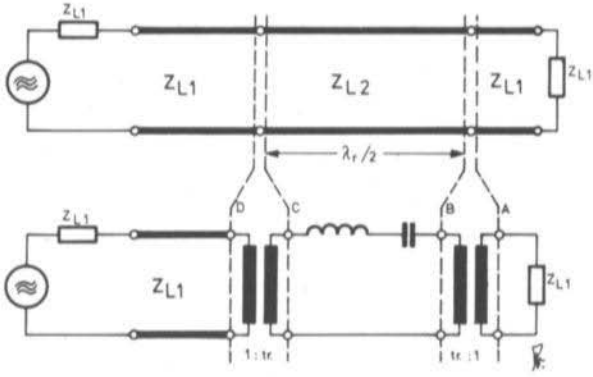

Fig. 22: Principle of a bandpass resonator with equivalent diagram

Figure 23 allows the behaviour of the locus in the vicinity of resonance to be calculated and proved.

Frequency $f < f_R$; $\lambda > \lambda_R$; $1/\lambda < 1/\lambda_R$

The angle $2\beta' l < 2\beta_r l$ is smaller. Point C' is within the capacitive half-plane at $|Z_C'| / Z_L > |Z_C| / Z_L$. D' is then on the φ-curve of C' at $|Z_D'| / Z_L = 5 \times |Z_C'| / Z_L$ frequency $f > f_R$, $\lambda < \lambda_R$: $1/\lambda > 1/\lambda_R$.

The angle $2\beta'' l > 2\beta_R l$ is greater. Point C'' is within the inductive half-plane at $|Z_C''| / Z_L > |Z_C| / Z_L$ so that D'' is also inductive.

This method allows the locus of the filter to be traced point for point (Fig. 23).

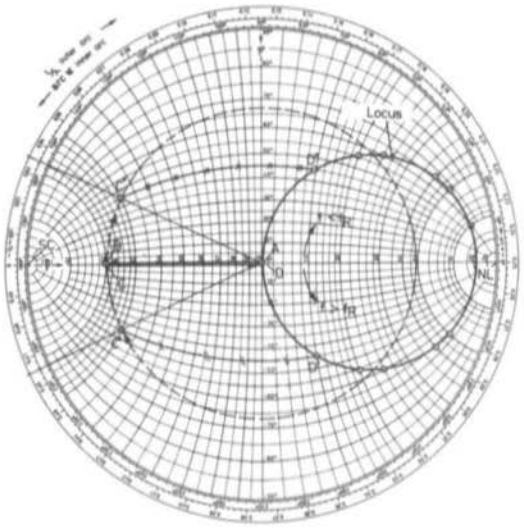

Fig. 23: Transformation path and theoretical locus of the bandpass resonator

The filter was built up and its locus in the input plane was measured using a measuring line. The frequency behaviour corresponded to the calculations. However, the resonant frequency was 1215 MHz and not 1300 MHz.

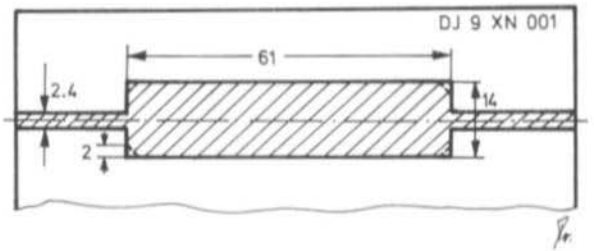

Fig. 24: Dimensions of a microstripline filter for 1300 MHz

This deviation of f_R of approximately 6% could have be caused by the following:
a) Inaccurate curves (5% tolerance is given in (4)).
b) Inaccurately known ε_r.
c) The corners of the $\lambda/2$ resonator were not compensated by tapering them. This leads to extra capacitance which will lower f_R.

The four corners of the resonator were removed experimentally (Figure 24) and the input impedance measured once more. The resonant frequency was now shifted to approximately 1235 MHz (error $\Delta f/f_R < 5\%$) which proves the importance of possibility c) above.

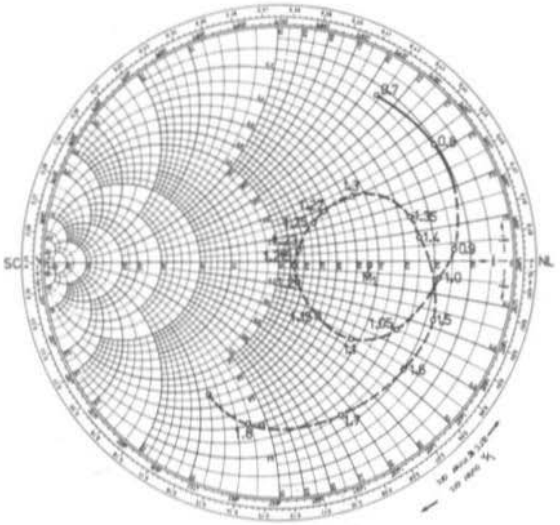

Fig. 25: Measured locus of the input impedance of the 1300 MHz microstripline filter

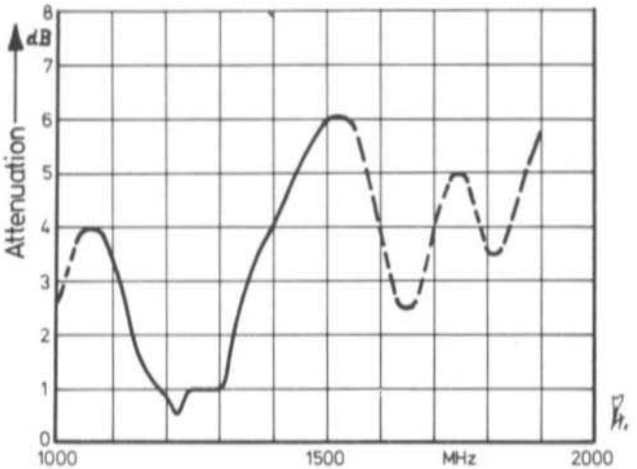

Fig. 26:
Insertion loss of the 1300 MHz microstrip filter

6.3. COMPUTATION OF A SINGLE-STAGE PREAMPLIFIER FOR THE 70 cm BAND

6.3.1. OUTPUT MATCHING

The output of a transistor stage with the values G = 1 mS, C = 2 pF at λ_R = 69.1 cm is to be matched to a real load of 1/G 2 60 Ω. The transformation is to be made as shown in Fig. 27. The load is galvanically coupled to a short-circuit line circuit with a line of Z_L = 60 Ω (w/h = 1.25; w = 1.88 mm). Required are the lengths l_1, l_2 and the impedance of the line circuit at the load conductance G_2 and the internal conductance $Y_i = G_i + jB_i$. Since the transformation path is prescribed, a fixed relationship exists between l_1 and l_2 which is only dependent on Z_L. This means that it is necessary to select Z_L before l_1 and l_2 can be computed.

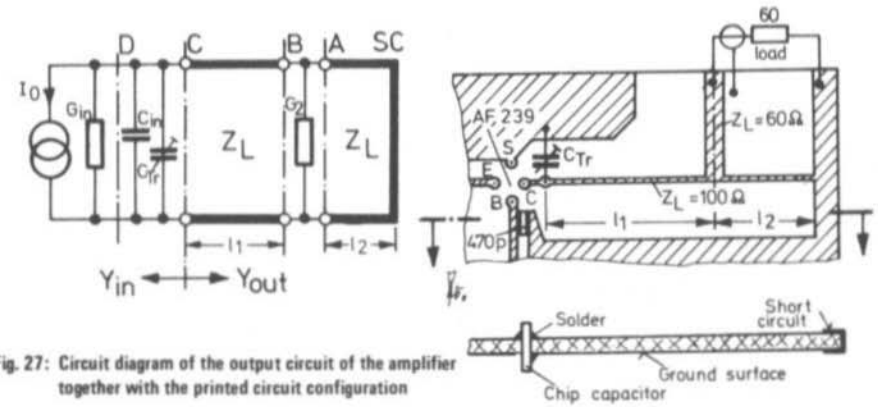

Fig. 27: Circuit diagram of the output circuit of the amplifier together with the printed circuit configuration

It will be seen in the Smith diagram given in Figure 28 that the /r/-curve passes through the point $g_i = G_i \times Z_L$, $b = 0$ and must intersect the G-curve $g_2 = G_2 \times Z_L$ so that it is possible to carry out a transformation with the described circuit. The magnitude g' is obtained by rotation of g by $180^\circ \triangleq \lambda/4$. This corresponds mathematically to the following when using equation (2) for $l = \lambda/4$:

$$Z'/Z_L = Z_L/Z; \quad 1\,(G' \times Z_L) = G \times Z_L; \quad 1/g' = g$$

(see the g-values in the Smith diagram)

The intersection condition for the two curves is as follows:

$$g' \geq g_2$$

The following is then derived:

$$1/(G' \times Z_L) > G_2 \times Z_L; \quad 1/(G \times G_2) > Z_L^2;$$

$$Z_L < \frac{1}{\sqrt{G_i \times G_2}} \rightarrow Z_L < \sqrt{6} \times 10^2\,\Omega \approx 240\,\Omega$$

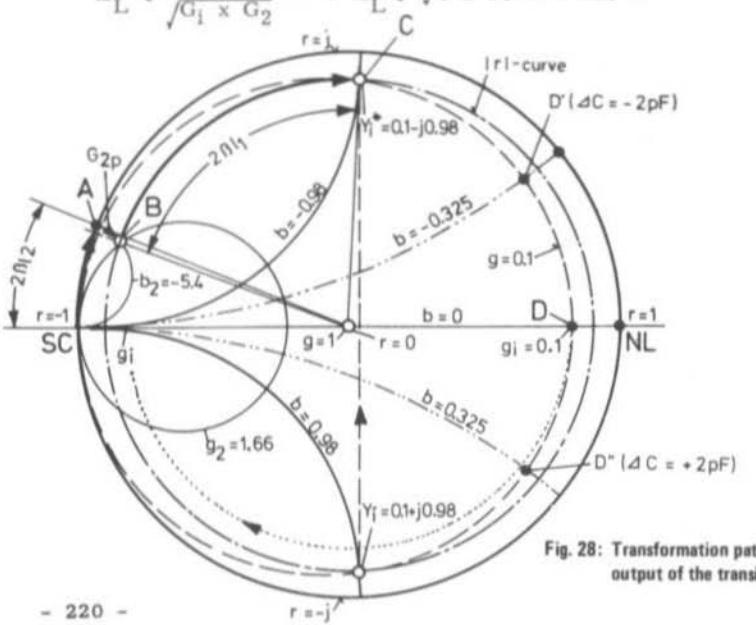

Fig. 28: Transformation path for the matching of the output of the transistor to 60 Ω

The most favourable even value that fulfils this condition and allows easy calculation is $Z_L = 100\,\Omega$, (w/h = 0.4; w = 0.6 mm); $\lambda_{st} = 0.635 \times \lambda_o$.

Values:

$G_2 = 1/60\,\Omega = 16.6$ mS; $g_2 = G_2 \times Z_L = 1.66$
$G_i = 1$ mS; $g_i = G_i \times Z_L = 0.1$

$C_{Tr} \pm \Delta C = 4$ pF ± 2 pF
$B_i = \omega (C_i + C_{Tr}) = 16.38$ mS ± 5.5 mS
$b_i = B_i \times Z_L = 0.98 \pm 0.325$
$y_i = g_i + jb_i$

Matching is provided when the following is valid:

$Y_{out} = Y_i^+$; $Y_i^+ = G_i - jB_i$

e.g. 1) $G_{out} = G_i$
2) $B_{out} = -B_i$

The point Y_i is firstly to be found in the Smith diagram after which Y_i^+ is obtained by mirroring against the real axis. This means that the final point of the transformation (C) has been determined from which the transformation can be carried out inversely:

A line of length l_1 ($= \lambda \times 0.1$; $l_1 = 4.4$ cm) rotates from plane B to C around the angle $2\beta l_1$. $G_2 \times Z_L$ is constant at B which means that B is the intersection of the /r/-curve through Y_i^+ with the G_2-curve.
B : 1.66 - j 5.4

Remove G_2, e.g. go to curve g = 1.66 - 1.66 = 0. This is the intersection A of the g-curve g = 0 (circumference of the Smith diagram) with the b-curve through B (b = -5.4). It will be seen that A is : 0 -j 5.4.

The line l_2/λ transforms from short circuit SC to point A ($l_2 = \lambda \times 0.029$; $l_2 = 1.27$ cm).

To finalize the output matching, let us consider the transformation process in the forward direction:

Planes	Type of circuit	Transformation on curve
SC → A	Line l_2	/r/ = 1
A → B	Parallel connection of G_2	b-curve (b = -5.4) to g = 1.66
B → C	Line l_1	/r/ < 1
C → D	Parallel connection of C_i and C_{Tr}	g-curve (g = 0.1) to b = 0 $\pm$ 0.325

Points C, D' and D'' can be adjusted with capacitance variations of ± 2 pF. The capacitance variation is large enough to achieve matching in the range of 430 to 440 MHz.

6.3.2. INPUT CIRCUIT

Required is the most simple, low-loss tranformation network between the input connector ($Z_{in} = 60\,\Omega$) and the input conductance of a transistor AF 239. The characteristics of the AF 239 at 450 MHz are as follows:

U_{CB} = -12 V; I_C = -2 mA in common base circuit $Y_{11} \approx$ 10 mS -j 30 mS, measured 5 mm under the case. If Z_L is selected as 60 Ω, the following values will be obtained:

$g_{in} = G_{in} \times Z_L = 1$; $g_{11} = G_{11} \times Z_L = 0.6$; $b_{11} = B_{11} \times Z_L = -1.8 \rightarrow$ point A

Theoretically speaking, there are an infinite number of ways to move the point $Y_{11} \times Z_L$ in the Smith diagram to the matching point.

The shortest path is provided by three circuits each having two reactive elements or a line. These circuits are given in Figure 29 together with their transformation diagram. It is advisable with all three circuits for the capacitances to be provided as trimmers so that alignment is possible. It is also possible for the parallel capacitance to be obtained using a stub line which can also be used as DC connection. The series capacitances also serve to isolate the DC-circuits from the input connector.

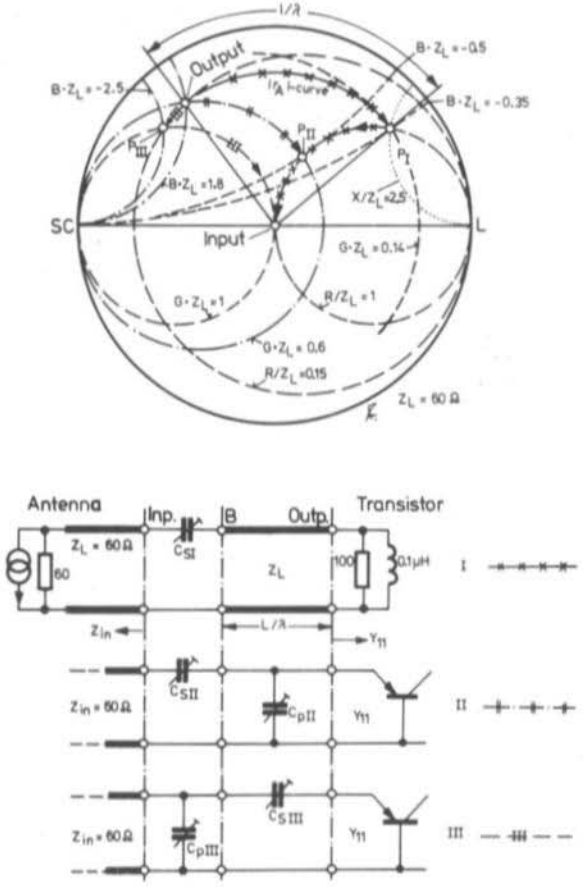

Fig. 29: Three transformation circuits for matching the antenna to the input of the amplifier

Description of the selected solutions with table of values for Figure 29.

Circuit	Step	from	Transformation on curve ...	to point	Y-coordin.	Z-coordin.	Arc length l/λ
I	1	Outp.	$/r/$=const.	P_I	0.14-j 0.35	1 + j2.5	0.123
	2	P_I	R/Z_L 1	Input	$1 \pm j0$	$1 \pm j0$	
II	1	Outp.	g_{11}=const=0.6	P_{II}	0.6 - j 0.5	1 + j0.8	
	2	P_{II}	$R/Z_I = 1$	Input	$1 \pm j0$	$1 \pm j0$	
III	1	Outp.	$R/Z_L = 0.15$	P_{III}	1 - j2.5	0.15 + j0.35	
	2	P_{III}	g_{in} = const.=1	Input	$1 \pm j0$	$1 \pm j0$	
				Outp.	0.6-j 1.8	0.15 + j0.475	

It should be mentioned how one obtains the Z-coordinates of a point when using a Y-diagram and not wishing to use a new sheet. The coordinates Y x Z_L will be transposed to Z/Z_L by rotating each point in the diagram by 180° around the centre point r = 0. The auxiliary point mirrored from the centre point is marked with compass and ruler and its coordinates are noted (Do not forget to observe the sign reversal of the reactive component). Finally, the transformation paths are carried on in the original half-plane.

Evaluation of Figure 29: $Z_L = 60\ \Omega$, $\lambda_o = 69.1$ cm

Circuit I:

$l/\lambda_{st} = 0.123$; $w/h = 1.25$, $w = 1.88$; $\lambda_{st}/\lambda_o = 0.595$

$\lambda_{st} = 41.1$ cm; $l = 5.05$ cm

$$\frac{X_{cs}}{Z_L} = \frac{X_{pI}}{Z_L} - \frac{X_{in}}{Z_L} = 2.5; \quad X_{cs} = 2.5 \times Z_L = 150\ \Omega$$

$$X_{cs} = \frac{1}{\omega_{cs}} \qquad C_s = 2.5\ \text{pF}$$

Circuit II:

$b_{cp} = b_{pII} - b_{out} = -0.5 - (-1.8) = 1.3$

$b_{cp} = B_{cp} \times Z_L = \omega c_{pII}$

$\omega C_{pII} = 1.3/Z_L = 1/46\ \Omega$

$C_{pII} = 8$ pF

$X_{csII}/Z_L = X_{pII}/Z_L - X_{in}/Z_L$

$X_{csII} = 0.8 \times Z_L = 48\ \Omega$

$X_{csII} = 1/\omega_{csII}$

$C_{sII} = 7.7$ pF

Circuit III:

$X_{csIII}/Z_L = X_{out}/Z_L - X_{pIII}/Z_L$

$X_{csIII}/Z_L = 0.475 - 0.35 = 0.125$

$X_{csIII} = 0.125 \times Z_L = 7.5\ \Omega$

$C_{sIII} = 49$ pF

$b_{cpIII} = b_{in} - b_{pIII} = 2.5$

$\omega C_{pIII} = 2.5/Z_L = 1/24\ \Omega$

$C_{pIII} = 14.5$ pF

6.3.3. PRACTICAL CIRCUIT

Circuit I is more favourable for use as an amplifier at frequencies in excess of 1 GHz since the length $l = 5.0$ cm at 434 MHz is difficult to construct and accommodate. Unfavourable lengths will also result if the parallel capacitance in circuit II is to be realized by use of a stub line (Table 3). Circuits II and III can be equally well constructed using trimmer capacitors. The longitudinal capacitances serve to isolate the voltage between input and emitter.

Table 3: Realization of the parallel capacitance C_{pII} by use of a stub line:

Z_L	λ_{st}	w	C_p	$b_{cp}=B_{cp}xZ_L$	$1/\lambda_{st}$	l
60 Ω	40 cm	1.88 mm	8 pF	1.3	0.413	16.5 cm
12 Ω	36.6 cm	15 mm	8 pF	0.26	0.29	10.6 cm

A printed circuit board was constructed for the amplifier in order to check the correctness of the calculated results. The amplifier uses the input circuit II. Special disc-shaped bypass capacitors without connection wires (chip capacitors) are used in the base and collector connections. The minimum spacing for the upper ground surface portions of greater than 5 w is maintained. Practical operation has shown that it is necessary for these ground surfaces to be provided with through contacts at several positions in order to avoid "hot points". The amplifier is connected to the coaxial antenna feeder and the sheathing is grounded directly under the stripline to the ground surface. The component values are given in a list later. It is necessary for the connection leads of the transistor to be shortened to approximately 6 mm in length, and fanned out by about 1 mm. This ensures an effective length of 5 mm from the transistor case to the conductor lanes. The connections of the resistors and capacitor C 6 are placed through the printed circuit board from the ground side. The operating voltage of the amplifier is 12 V. With the given component values, 10.6 V will be present at the emitter and 10.3 V at the base (measured against ground with a transistor voltmeter.

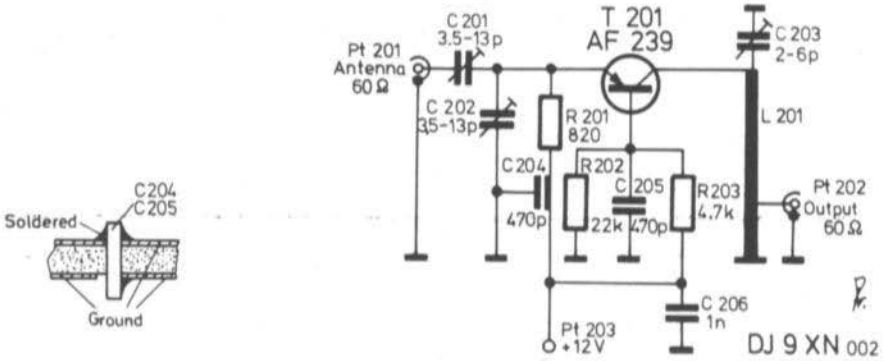

Fig. 30: Circuit diagram of the 70 cm preamplifier

Measured characteristics: Centre frequency 435 MHz
Gain 15 dB
Bandwidth 37 MHz
Loaded $Q = \frac{\omega r}{\Delta \omega} = 11.7$

Components: T 1: AF 239 (s)

C 201: 3.5-13 pF trimmer capacitor
C 202: 3.5-13 pF trimmer capacitor
C 203: 2 - 6 pF trimmer capacitor
C 204: 470 pF chip capacitor
C 205: 470 pF chip capacitor
C 206: 1 nF chip capacitor

R 201: 820 Ω; R 202: 22 kΩ; R 203: 4.7 kΩ

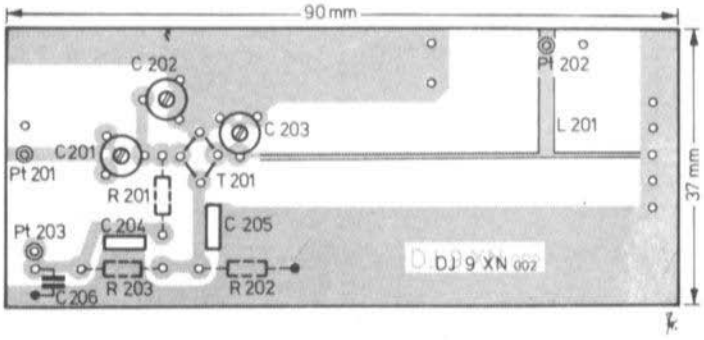

Fig. 31: Printed circuit board and component locations of the preamplifier

6.4. IMPROVED BANDPASS RESONATOR FOR 23 cm

As has already been explained, filter characteristics such as skirt slope are dependent mainly on the value of the impedance jump. It is possible for the transformation ratio $tr = \sqrt{Z_L'/Z_L}$ to be increased simply by increasing the number of impedance jumps from the two jumps in 6.2. A balanced filter is to be calculated that has an attenuation minimum at 1300 MHz. The graphical determination of the lengths is to be carried out according to the normal method (Fig. 33). The terminating impedance for the filter is 50 Ω up to plane A. Transition from $Z_{L1} = 50\ \Omega$ to the 10 Ω line: Plane A to B:

$$Z_B/Z_{L2} = Z_A/Z_{L2} = (Z_A/Z_{L1}) (Z_{L1}/Z_{L2})$$

$$Z_B/10\ \Omega = 1 \exp (j\,0^o) \times 5 = 5 \exp (j\,0^o)$$

Transformation on the 10 Ω line l_1/λ_{st}, step B-C on the /r/-curve in clockwise direction.

In order to allow the use of several approximation formulas, it is necessary for all lines to have a length of less than $\lambda/8$. This is the reason why a random length of $l_1/\lambda_{st} = 1/16$ has been selected. With $l_1/\lambda_{st} = 0.062$ one passes from Z_B to $Z_C/10\ \Omega = 2.2 \exp (-j\,59^o)$ in the Smith diagram.

Jump from 10 Ω to 90 Ω line: Plane C to D from point Z_C on the φ -curve -59^o to $Z_D/Z_{L3} = (Z_C/Z_{L2}) (Z_{L2}/Z_{L3})$;
$Z_D/90\ \Omega = 2.2 \exp (-j\,59^o) \times 1/9 = 0.244 \exp (-j\,59^o)$.

Transformation on the 90 Ω line from plane D to E whereby Z_E is a complex congruent to Z_D.

$$Z_E/90\ \Omega = Z_D/90\ \Omega = 0.244 \exp (+j\,59^o)$$

A further jump from plane E to plane F (10 Ω) is made:

$$Z_F/Z_{L2} = (Z_E/90\ \Omega)\ (90\ \Omega/10\ \Omega) = Z_C^+/10\ \Omega;\ Z_F/10\ \Omega = 2.2 \exp. (+j\,59^o)$$

The transition from F to G is made with a 10 Ω line of length l_1. The impedance in plane G is once again real 50 Ω at the resonant wavelength. The following 50 Ω line is connected without reflection in plane G.

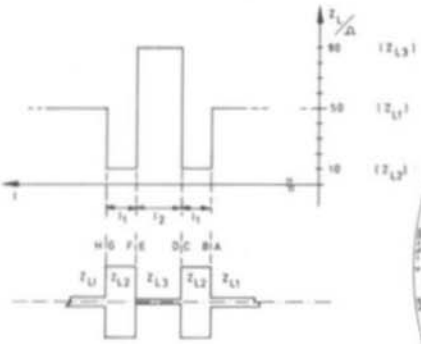

Fig. 32:
1300 MHz filter. Line impedance as a function of the line length and geometric structure. Designation of the transformation planes.

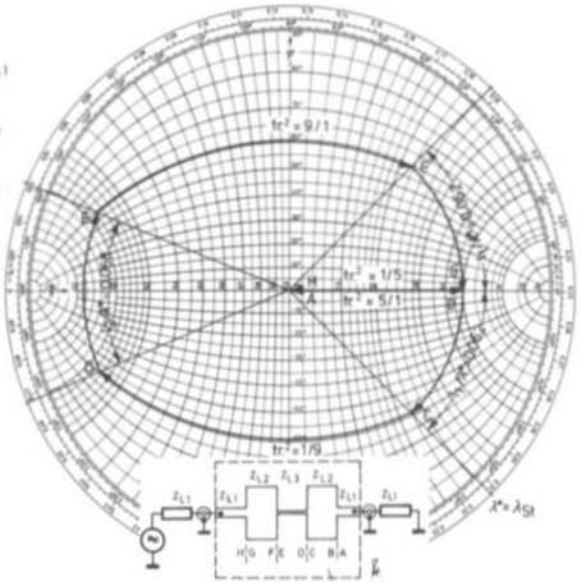

Fig. 33:

a) Computation of the length in a Charter diagram for the balanced bandpass filter for 1300 MHz using lines of 50, 10 and 90 Ω.

b) Prescribed line structure with external connections to the PC board

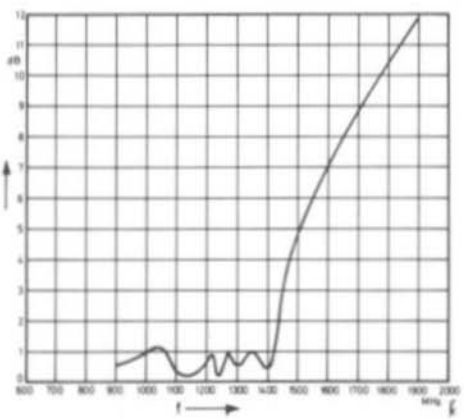

Fig. 34: Insertion loss of the 1300 MHz low-pass filter

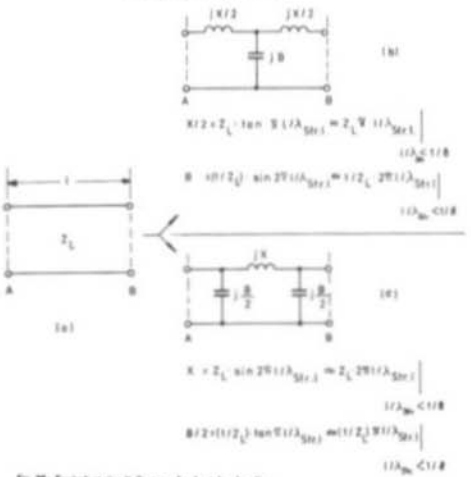

Fig. 36: Equivalent circuit diagram of a short, low-loss line

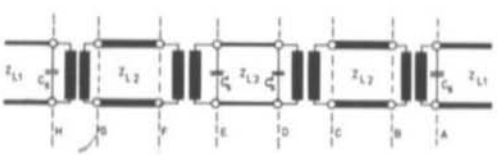

Fig. 35:
Line equivalent diagram of the 1300 MHz filter. The stray capacitances were neglected during the computation

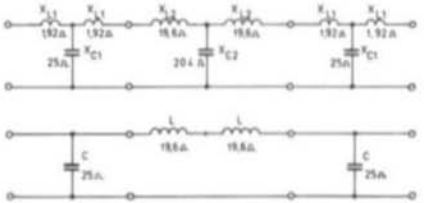

Fig. 37:
1300 MHz filter. Equivalent Π -circuit diagram with computed values of the components according to Fig. 36 after deducting the possible neglectable values

Table 4: List of the filter dimensions, evaluation of Figure 33.

	$\frac{\lambda_o}{cm}$	w/h	$\frac{w}{mm}$	λ_{st}/λ_o	$\frac{\lambda_{st}}{cm}$	$1/\lambda_{st}$	1/mm
$Z_{L1} = 50\,\Omega$	23	1.75	2.45	0.585	-	as requ.	as requ.
$Z_{L2} = 10\,\Omega$	23	≈ 12	≈17	0.525	12.1	0.062	7.5 $\varepsilon_r = 5$
$Z_{L3} = 90\,\Omega$	23	0.52	0.73	0.625	14.38	0.068	9.8, h = 1.4 mm

The measurement of the insertion loss (Fig. 34) indicated typical low-pass filter characteristics with a minimum attenuation pole of 0.2 dB at 1240 MHz. The frequency shift is due to ignoring the stray capacitances. The measured characteristics are not surprising when one considers the line configuration. When it is assumed that the 10 Ω line has the effect of a parallel capacitance and the narrow 90 Ω line as a series inductance, the simplified equivalent diagram would have the form of a low-pass π-filter. If some magnitudes can be neglected, it will then be possible to compute the cutoff frequency of the low-pass filter:

A line can be replaced by a π or T-link, constructed from inductances and capacitors (Fig. 36), if the following prescriptions are fulfilled:

1) Length of the line is less than $\lambda_{st}/8$.
2) Low loss line.
3) Inductance component L' = L/l and the capacitance component C' = C/l should be constant in the frequency range of interest to which the cutoff frequency belongs.
4) Low and high impedance must alternate on the lines.

The stray capacitances between the lines that are generated by the distortion of the electrical field lines are ignored in the computation: It is not possible to know what other elements of an equivalent diagram can be ignored until all X-values have been computed.

The lines of the filter are now replaced by equivalent T-circuits and the elements are computed according to the formulas given in Figures 36 and 37, as well as Table 4.

The 90 Ω-line possesses the lowest capacitive component and thus the highest impedance X_{C2}. It is possible for X_{C2} to be ignored since many smaller X-values are effective in parallel. However, it is not possible to ignore X_{C1} since it is expecially these capacitances that load the input of the filter to a large extent. The series inductances of $X_{L1} = 1.9\,\Omega$ are only of minor importance in comparison with the loading of X_{C1} (X_{L1}: $X_{C1} \approx 2 : 25$) and may therefore be ignored. When the previously mentioned values are neglected, a conventional single-link low-pass filter with the elements 2 L and C remaining will result, whose cutoff frequency f_c (insertion loss 3 dB) can be determined as follows:

$$\omega_c = \frac{1}{\sqrt{LC}} = 2\pi \times f_c$$

If equation (11) is extended by the operating frequency $\omega = 2\pi f$, the following equation will be obtained

$$f_c = \frac{f}{\sqrt{X_L/X_C}}$$

which, when used with our filter, results in the value:

$$f_c \approx \frac{1300 \text{ MHz}}{\sqrt{19.6\ \Omega / 25\ \Omega}} = 1460 \text{ MHz}$$

The coincidence between the theoretical and practical value of the cutoff frequency is extremely good. However, this cannot be assumed to be always the case.

REFERENCES TO PART II

(6) RCA: Semiconductor Circuits in Power Electronics (1971)

(7) RCA: Application Notes on RCA Transistors (1971)

(8) Prof. Dr. H. Friedburg: Mikrowellenmesstechnik
Vorlesungsskriptum 1970/1971, University of Karlsruhe, Germany

(9) H. Sobol: Applications of Integrated Circuit Technology to Microwave Frequencies
Proceedings of the IEEE, Vol. 59, No. 8, August 1971

(10) Mattaei, Young, Jones: Microwave Filters, Impedance Matching Networks and Structures
Mc Graw - Hill Book Company, New York

(11) Caulton, Hughes and Sobol: Measurements on the Properties of Microstrip Transmission Lines for Microwave Integrated Circuits
RCA Review, Sept. 1966

MODIFICATION to the SYNTHESIS VFO DL 3 WR 007

The variable capacitor of the original VFO had a capacitance variation range of 150 pF and not 100 pF.
Since it has not been possible for us to obtain a high-quality 150 pF variable capacitor, the following modifications should be made in order to obtain the full frequency variation range of 333 kHz:

Increase the inductivity of L 1 by placing a small inductance in series with the supplied 2.5 uH coil so that the total inductance is increased to 4.1 µH.

Increase the total capacitance of C 3 / C 4 / C 5 to 510 pF. Styroflex caps. can be used instead of the mica types. Suitable values are: C 5 = 440 pF, C 4 = 46 pF, C 3 = 30 pF air-spaced trimmer. If L 1 is to be wound, the 4.1 µH can be obtained with the following:
22 turns enamelled copper wire of 0.5 mm dia. (24 AWG) wound on a ceramic coil form of approx. 14.3 mm dia. Coil length 18 mm, without core.

Very 73 de VHF COMMUNICATIONS and UKW-BERICHTE

FURTHER DEVELOPMENT OF THE FOUR-DIGIT FREQUENCY COUNTER

by F. Weingärtner, DJ 6 ZZ

The four-digit counter module for 30 MHz (1) has been further developed with the aid of two new integrated circuits that allow the upper frequency limit to be increased to at least 50 MHz, and typically 70 MHz. In addition to this, the new printed circuit board has been designed to accommodate the smaller indicator tubes that are directly soldered into the PC-board. This new type of "Nixie" tubes have the same size of digit but are only approximately half the size of the previous types. They are also provided with two decimal points.

Figure 1 shows the prototype set-up in conjunction with the preamplifier/pulse shaper module DL 8 TM 001 (2) which is suitable for operation in the frequency range of 200 kHz to 80 MHz and can be driven by an input voltage of approximately 50 mV.

Since the 1 MHz crystal oscillator and frequency dividers are part of the counter module, the unit will be completed by provision of a power supply, e.g. such as described in (3). This simple and compact four-digit frequency counter with its resolution of 100 Hz is especially suitable for use as digital frequency readout in conjunction with transmitters and receivers. The extended frequency range allows not only the short-wave bands to be directly read off but also the 50 MHz and 70 MHz amateur bands. Besides this, it provides the possibility of directly measuring the frequency of the crystal oscillator and subsequent frequency multipliers so that the frequency of 2 m and 70 cm equipment can be measured accurately, even though the counter is not able to indicate the actual output frequency.

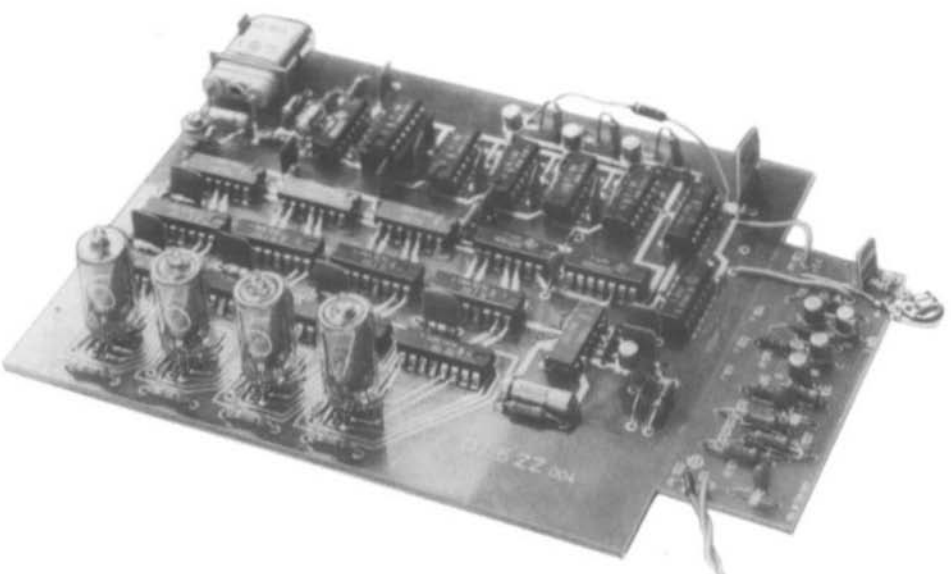

Fig. 1: Photograph of the author's prototype

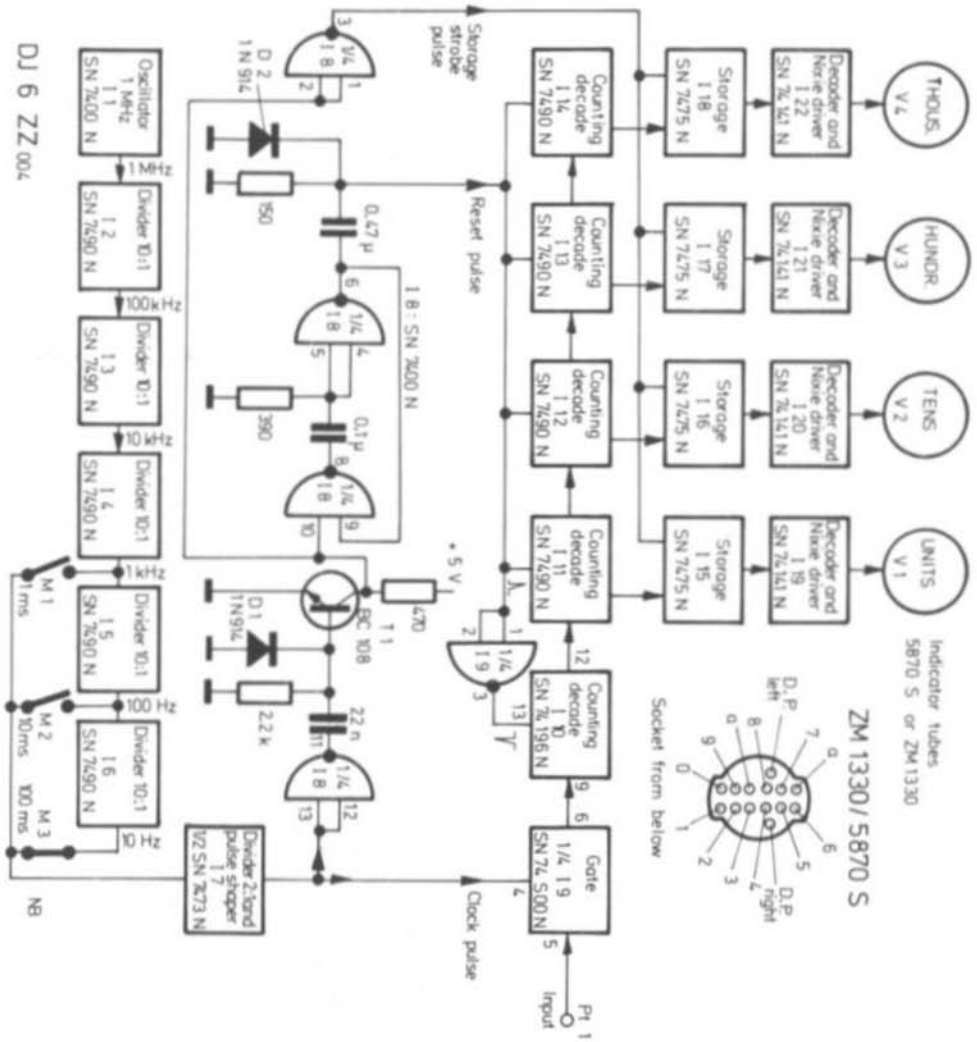

Fig. 2: Block diagram of the 4-digit counter DJ 6 ZZ 004

1. CIRCUIT MODIFICATIONS

As can be seen in the block diagram of the frequency counter DJ 6 ZZ 004 given in Figure 2, the following differences can be seen when comparing it to the original DJ 6 ZZ 003 module: The new, miniature indicator tubes type 5870 S or ZM 1330 are used. The switches for the built-in decimal points have not been drawn in the diagram. A second wafer on the measuring time switch M 1 to M 3 can be used for this. The decimal points will light up when the indicator tube connections "D.P." are grounded.

In the first counting decade I 10, the counter SN 7490 N has been replaced by type SN 74196 N. The upper frequency limit of this type is given as being at least 50 MHz, typically 70 MHz. Since this decade counter requires a negative going reset impulse, one of the four gates of I 9 is connected as reversal stage in front of the reset input.

The gate (I 9) has also been simplified and matched to the higher counting frequency by use of a Schottky-TTL multiple gate SN 74 S 00 N. A single gate (connections 4, 5, 6) of I 9 operates as counting gate. The remaining two gates remain unconnected. If required, they can be used for regeneration of distorted input pulses.

The working resistor connected to +5 V required for the previously used simple pulse shaper circuit is no longer required for this preamplifier pulse shaper module.

Two critical points of both the previous and this frequency counter should be mentioned:

The crystal oscillator does not oscillate readily with all SN 74 00 N types. If difficulties are encountered, I 1 should be exchanged.

The inputs for the storage strobe pulse (I 15 to I 18, connections 4 and 13) represent together an input load factor of 16. If all 4 storage ICs accidentally obtain the maximum value, the gate I of I 8, (connections 1, 2, 3) will be overloaded, since the output load factor can only amount to 10. For this reason, attention should be paid that no secondchoice IC types are used. If one finds that this problem is not solved after exchanging the IC, it is suggested that the power-gate SN 7437 N should be used for I 8.

2. CONSTRUCTION

In order to ensure that the further development of the frequency counter can be constructed easily, the original PC-board has been redesigned and matched to the new indicator tubes and input circuit. Figures 3 and 4 show the new printed circuit board DJ 6 ZZ 004 and the component locations.

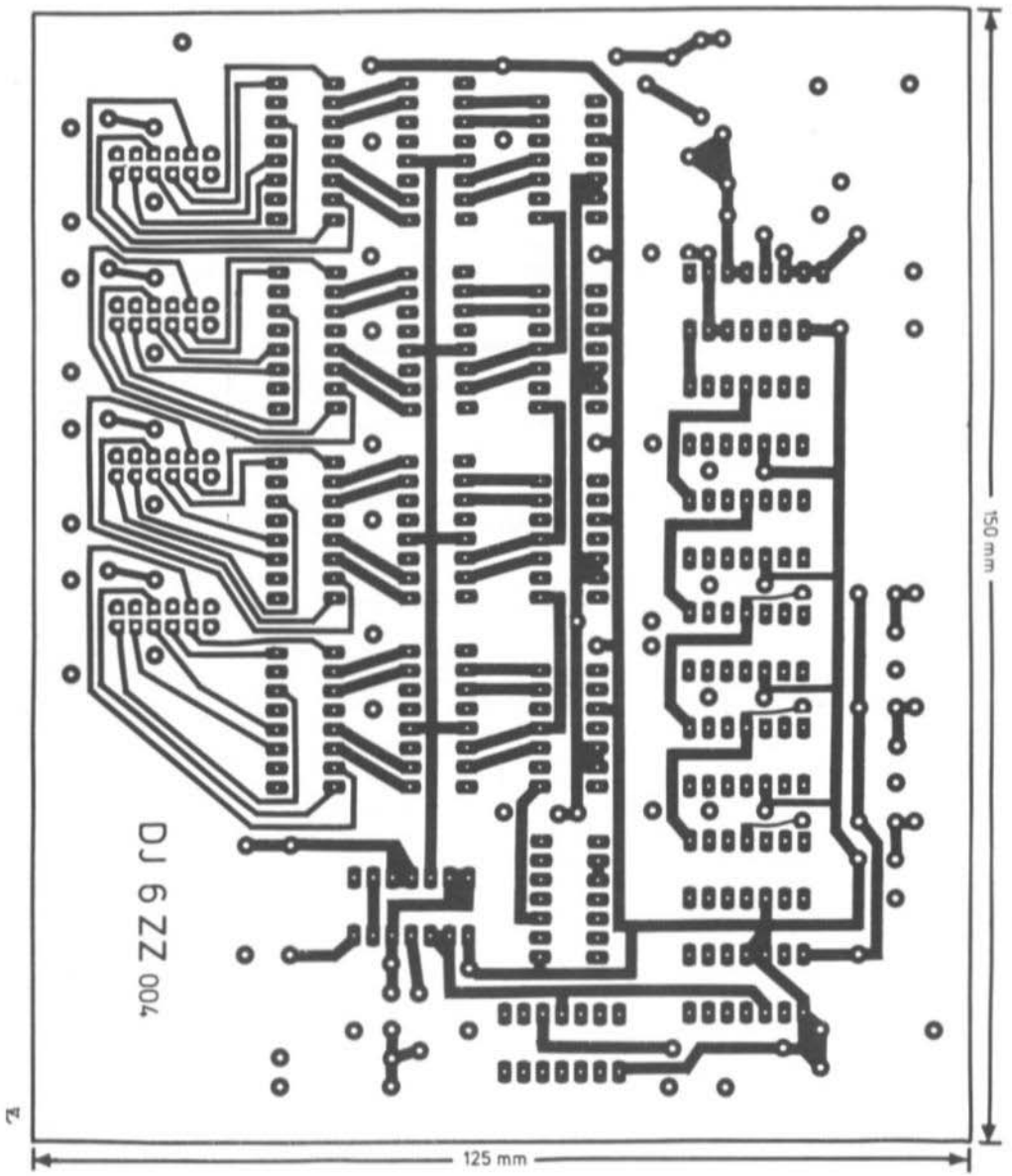

Fig. 3: PC-board DJ 6 ZZ 004; double-coated with through contacts

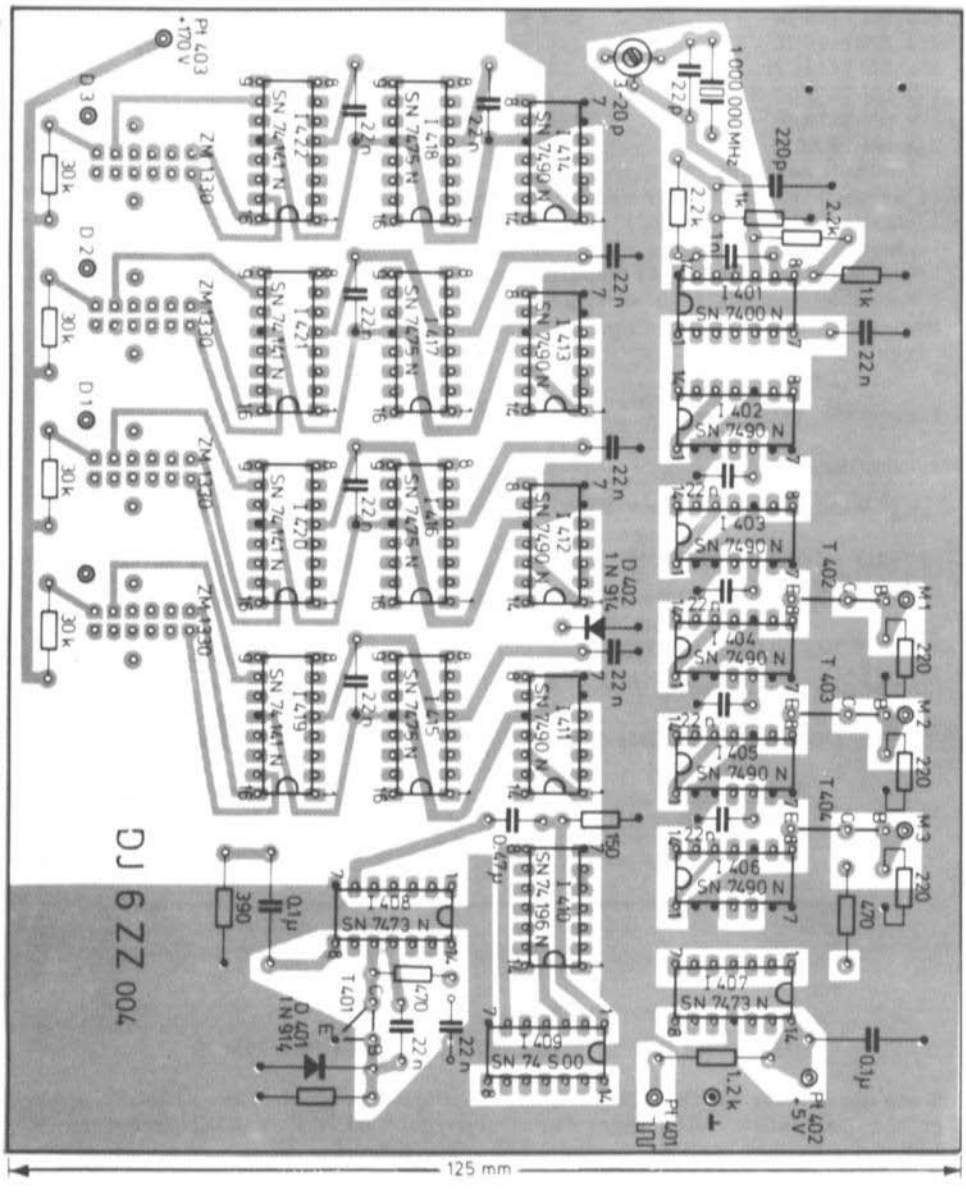

Fig. 4: Component locations to DJ 6 ZZ 004

2.1. COMPONENTS

4 x 5870 S (ITT) or ZM 1330 (Siemens)
4 x SN 74141 N
4 x SN 7475 N
9 x SN 7490 N
1 x SN 74196 N
1 x SN 74 S 00 N
1 x SN 7473 N
2 x SN 74 00 N
4 x BC 108 or similar
2 x 1 N 914 or similar
1 standard crystal 1.0 MHz, HC-6/U
1 horizontal crystal holder
1 trimmer 3 - 20 pF
1 ceramic capacitor 22 pF
1 styroflex capacitor 220 pF
1 ceramic capacitor 1 nF
14 ceramic capacitors 22 nF
1 plastic foil capacitor 0.1 μF (at I 8/8)
1 plastic foil or ceramic capacitor 0.1 μF (or more)
1 ceramic, plastic foil or tantalium capacitor 0.47 to 1 μF (at I 8/6)
1 tantalium capacitor 10 to 47 μF (at I 8/14)
Resistors, partly with 10 mm and 12.5 mm spacing.

3. AVAILABLE PARTS

Please see price list.

4. REFERENCES

(1) F. Weingärtner: A Four-Digit Frequency Counter Module for Frequencies up to 30 MHz
VHF COMMUNICATIONS 3 (1971), Edition 3, Pages 159-171

(2) W. R. Kritter: A Wideband Preamplifier for Frequency Counters up to 60 MHz
VHF COMMUNICATIONS 3 (1971), Edition 3, Pages 156-158

(3) H. Kahlert: Universal Power Supply Using an Integrated DC-Voltage Stabilizer
VHF COMMUNICATIONS 3 (1971), Edition 2, Pages 121-126

CW CALLING FREQUENCY AND CALLING TIMES

Since the number of VHF CW stations is relatively small, the VHF-DX group of the Darmstadt ARC suggests an international CW calling frequency of 144.050 MHz and calling periods from the full hour to five minutes after.

This is to be valid for every day and especially during the special activity days (Tuesdays). Using this system it may even be possible to find a QSO partner before going to work as this time often provides above average conditions DJ 2 RE, DJ 5 DT.

A STABLE CRYSTAL-CONTROLLED OSCILLATOR IN THE ORDER OF 10^{-7} FOR FREQUENCY AND TIME MEASUREMENTS

by R. Görl, DL 1 XX and B. Rößle, DJ 1 JZ

A 1 MHz crystal oscillator is to be described which exhibits a frequency error of better than $\pm 1 \times 10^{-7}$ when used in conjunction with a crystal oven. The circuit has been designed so that a good frequency stability is also obtained without oven. Fluctuations of the operating voltage and load have a very low effect on the frequency. Measured values are given with respect to the behaviour after switching on and during long periods of operation as is the effect of fluctuations of the operating voltage and load.

The oscillator circuit is provided with a varactor diode which allows fine adjustment of the frequency, and the synchronization of the oscillator when using the standard frequency receiver DJ 4 BG 010 (1). This means that several dif ferent versions are possible that can be selected according to the required frequency stability. The stability obtained using the crystal oven without synchronisation to a standard frequency transmitter should be underlined. It is not only the short-time stability obtained by use of the thermostat that is good but also the long-time stability since the aging of the crystal is very low due to the extremely low loading of the crystal itself.

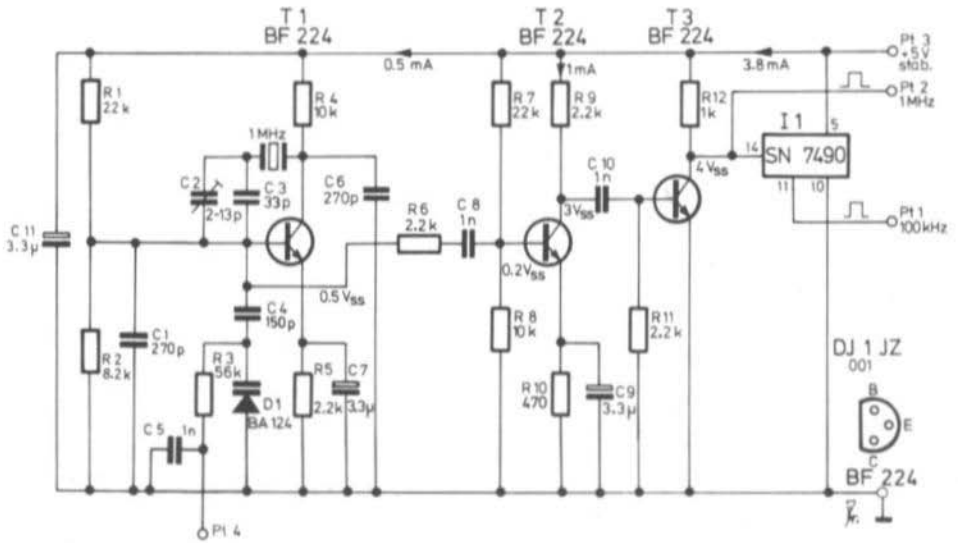

Fig. 1: Circuit diagram of the 1 MHz timebase with buffer, pulse shaper and 10 : 1 divider

1. CIRCUIT DETAILS

Figure 1 gives the circuit of the crystal time base. It includes the oscillator (T 1), a buffer amplifier stage (T 2), a pulse shaper (T 3) and an integrated frequency divider. The whole circuit operates with a stabilized operating voltage of 5 V, which is also required for the TTL-ICs of the equipment to be driven by the oscillator (electronic clock, frequency generator, counter etc.). The

transistors BF 224 are very low-reactive types; however, the circuit is very uncritical so that other types can be used.

One very favourable feature of this Pierce-circuit is the large capacitances in parallel with the base-emitter path and collector-emitter path of the oscillator transistor T 1. They are placed in parallel to the temperature and voltage-dependent transistor capacitances and thus reduce the effect of fluctuations of the ambient temperature and operating voltage. The capacitors C 1 to C 4 and C 6 must, of course, have a neutral temperature coefficient. The design of this circuit, in conjunction with the low operating voltage, means that the loading of the crystal remains less than 200 μW. This means that it is not necessary for a control circuit to be used for stabilization of the amplitude.

2. DIFFERENT VERSIONS

The crystal-controlled time base shown in Figure 1 can be built up in various versions according to the required frequency stability. A few possibilities are to be given in the following table:

Crystal oven	200 kHz RX	Crystals	Notes
1 no	no	XS 6002	Inexpensive calibrating crystal
2 no	no	XS 0604	More expensive crystals possible
3 XT-1/2	no	XS 0605/75°	Available crystal oven for 75°C
4 no	DJ 4 BG 010	XS 6002	See reference (1)
5 XT-1/2	DJ 4 BG 010	XS 0605/75°	High accuracy even when the standard frequency is not being transmitted

The crystal types given in the above table are manufactured by KVG and are available from the publishers. The 1 MHz standard crystals are now given in order of increasing accuracy:

Type	Total tolerance		Holder
	from +15 to +45 °C	at 25 °C	
XS 6002	$\pm$ 50 x 10^{-6}	alignm. tol. = $\pm$10 x 10^{-6}	HC-6/U, airtight sealed

Type	Alignment tolerance	Temperature response of the frequency f/fo	in the range	Holder
XS 0604	$\pm$10 x 10^{-6}	$\pm$10 x 10^{-6}	-20 to +70 °C	HC-6/U, sealed in a crystal oven (e.g. 75 °C)
XS 0605	$\pm$10 x 10^{-6}	$\pm$5 x 10^{-6}	$\pm$5° of the nominal temperature	

For the highest demands on the long-time stability and Q of the crystal, considerably more expensive types of crystals in evacuated glass holders (e.g. XS 3505) and cold-welded metal holder (e.g. XA 111) are available.

Crystal oven	XT - 1	XT - 2
Heater voltage	6 V	12 V
Heater current	1 A	0.7 A
Working temperature	75 $\pm$ 3 °C	
Control accuracy	$\pm$ 1 °C	
Control	Bimetal	
Connection socket	Octal	
Dimensions	overall height: 60 mm; diameter: 32 mm	

The following should be noted when the crystal oscillator is to be synchronized to the 200 kHz transmitter Droitwich: The field strength of this transmitter is very low in Southern Europe which means that only a very low signal-to-noise ratio is present. For this reason, it is necessary for the time constant of the control loop to be very long which can be obtained by using large capacitance and/or resistance values in the DC control voltage line. If this is not taken into consideration, atmospheric interference can cause an unwanted phase modulation of the crystal oscillator which will reduce the usability of the oscillator signal considerably.

3. CHARACTERISTICS AND MEASURED RESULTS

Circuit No. 3 equipped with the 12 V crystal oven XT-2 and the crystal XS 0605/75 °C was built up by DJ 1 JZ and measured by DL 1 XX. The measurements were carried out at an ambient temperature of 18 °C using a home-made frequency measuring system which included the frequency standard XSE of Rhode and Schwarz. The measuring resolution and absolute accuracy of this system is

$$\frac{f}{fo} \quad 1 \times 10^{-8}$$

Before carrying out the measurement, the oscillator was aged in continuous operation over a period of 14 days.

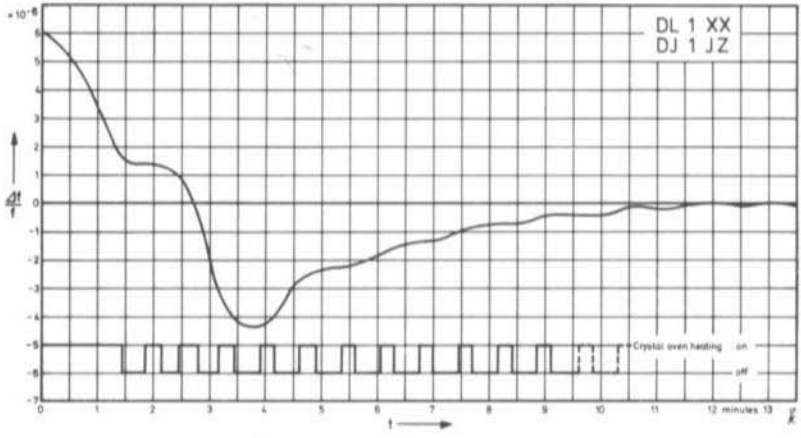

Fig. 2: Frequency behaviour on heating the thermostat

Figure 2 indicates the frequency variation on heating the crystal oven after switching on. The final temperature of the crystal and thus a frequency accuracy of better then $\pm 2 \times 10^{-7}$ is obtained after approximately 12 minutes. The switching cycles of the heating of the crystal oven are given below the frequency curve. Figure 2 allows the following conclusions: Since the direction of frequency drift reverses after approximately 3.7 minutes, whereas the crystal has not reached its final temperature due to its poor heat conductivity, the crystal will not be operating at its temperature reversal point. In this case, the crystal may possibly be a type selected according to its load capacitance corresponding to standard CR-18/U, whose temperature reversal point is too low. In a later measurement, this was found to be at 62 °C. However, this

is not always a disadvantage since the temperature coefficient of AT-cuts with a reversal temperature point of 75 °C - e.g. as with type CR-27/U - will be far less favourable if the reversal temperature is not exactly obtained with simple crystal ovens such as used here.

During continuous operation, periodic frequency variations will occur due to the temperature cycles of the crystal oven. These are given in Figure 3. The frequency error amounts to $\pm 1 \times 10^{-7}$.

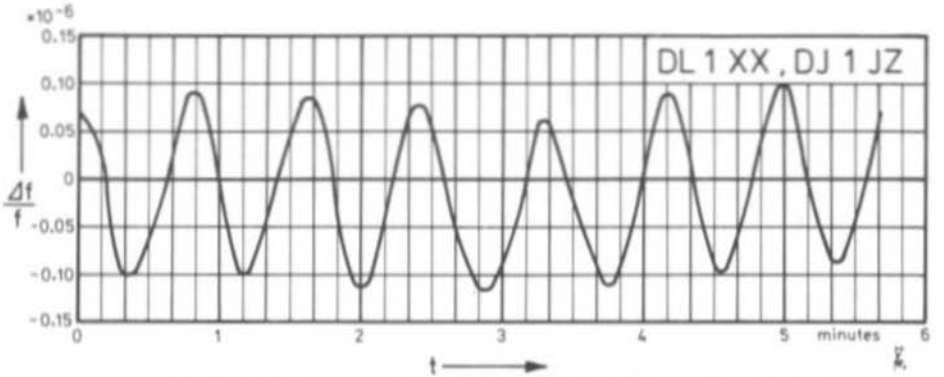

Fig. 3: Periodic frequency variations due to the temperature cycles of the crystal oven

The following frequency variations occur on changing the operating voltage U_B of the oscillator:

U_B	$\Delta f/fo$
4.5 V	-0.7×10^{-6}
5.0 V	0
5.5 V	$+1 \times 10^{-6}$

This results in approximately $\pm 1 \times 10^{6}/\pm 0.5$ V. This means that the operating voltage should not fluctuate by more than ± 0.05 V or be superimposed with a hum voltage. The integrated control circuit such as that given in (2) is suitable for use as power supply.

The frequency variation on short circuiting the 1 MHz output (Pt 3) to ground is: $\frac{\Delta f}{fo} < 10^{-8}$

The tuning range of the varactor diode amounts to 1.3×10^{-6} at a voltage variation between 0 V and 5 V. If this diode is not to be used, it should be connected to the stabilized operating voltage of 5 V. The diode can also be deleted and replaced by a wire bridge.

As has already been mentioned, the loading of the crystal amounts to 0.2 mW in this circuit which is sufficiently below the value of 0.5 mW which KVG lists as maximum loading for their precision crystals when high demands are placed on the long-time stability.

Finally, the equivalent data of the crystal were determined in a π-circuit according to German Industrial Standard DIN 45 105:

Crystals: XS 0605, 1 MHz, 75 °C
R 1 = 205 Ω ± 10%
L 1 = 3.0 H ± 10%
Q ≈ 90 000

Minimum impedance frequency: 999.8832 kHz

4. CONSTRUCTION

The circuit given in Figure 1 is accommodated on a 65 mm x 50 mm PC-board which has been designated DJ 1 JZ 001 and is shown in Figure 4. When the crystal oven is used, the crystal is no longer accommodated on the PC-board but in the crystal oven.

A photograph of the author's prototype is given in Figure 5. The two connections of the crystal are fed from the socket of the crystal oven to the connections on the PC-board. The two heater connections are fed to feedthrough capacitors placed into the walls of the TEKO case. The 1 MHz and the 100 kHz output are connected to low-capacitive feedthroughs whereas the operating and tuning voltage are fed in via feedthrough capacitors.

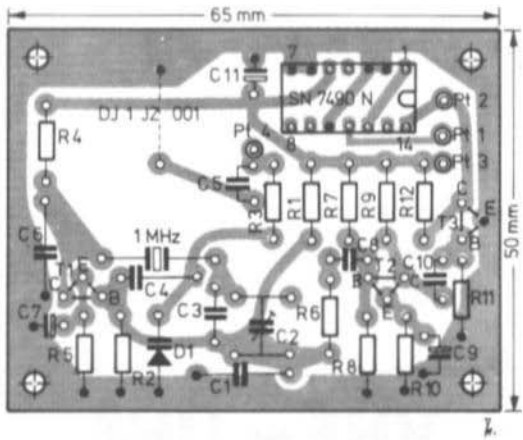

Fig. 4: PC-board DJ 1 JZ 001 and component locations

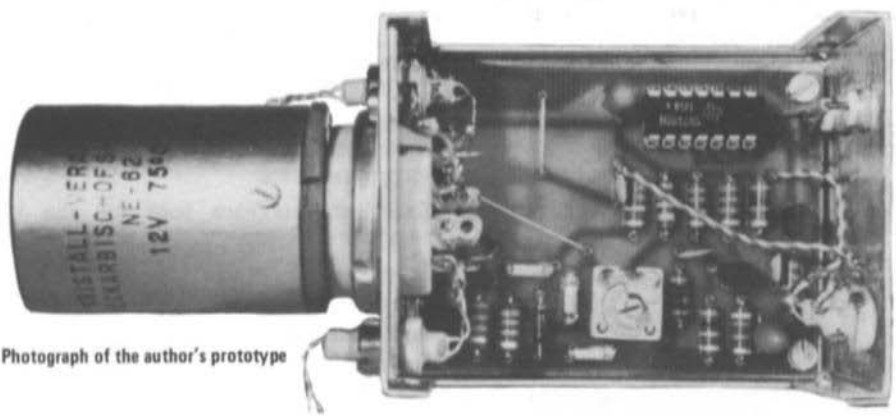

Fig. 5: Photograph of the author's prototype

4.1. COMPONENT DETAILS

T 1 - T 3: BF 224 (TI), BF 173, 2 N 3304 or similar RF types
D 1: BA 124, BA 125 (AEG-Telefunken), 1 N 5472 A or similar (approx. 50 pF)
I 1: SN 7490 N (decade counter) (Texas Instruments)

Crystal: See Section 2

C 1, C 6: 270 pF styroflex capacitor
C 2 : 2 - 13 pF air-spaced trimmer
C 3 : 33 pF ceramic capacitor TC 0
C 4 : 150 pF styroflex capacitor
C 5, C 8, C 10: approx. 1 nF ceramic capacitor, spacing 5 mm
C 7, C 9, C 11: 1 µF to 4.7 µF tantalium electrolytic capacitor, drop type

Crystal oven XT-1 or XT-2 for accommodation of max. 2 HC-27/U or HC-6/U crystals, connection diagram:

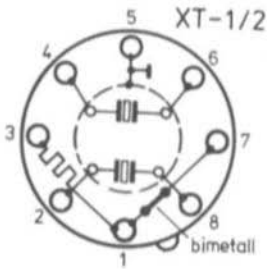

5. REFERENCES

(1) E. Schmitzer: A 200 kHz Receiver for Synchronizing 1 MHz Oscillators to the Droitwich Longwave Transmitter
VHF COMMUNICATIONS 4 (1972), Edition 2, Pages 111-118

(2) H. Franke and H. Kahlert: Universal Power Supply Using an Integrated DC Voltage Stabilizer
VHF COMMUNICATIONS 3, (1971), Edition 2, Pages 121-126

AMATEUR TELEVISION

Part II

by T. Bittan, G 3 JVQ/DJ Ø BQ

4. TELEVISION TRANSMISSION

4.1. INTRODUCTION

There are two main ways of combining the audio and video signal to form an ATV signal that can be resolved and heard in a conventional domestic TV receiver with appropriate converter. The first uses a separate UHF transmitter for video and sound which are combined in the final output stage or at the antenna. The other method is to combine the video and sound signals at IF level where the same frequency conversion and amplification is used for both signals. An ATV transmitter for 70 cm based on the latter principle is to be described in one of the next editions of VHF COMMUNICATIONS.

As was stated in (1), there are unfortunately still differences in the picture-sound carrier spacings and type of audio modulation at UHF. However, since FM modulation is more widespread and most domestic receivers for UHF are equipped for this mode, we will only deal with FM. The different picture-sound carrier spacings can be easily compensated for in the sound transmitter or by shifting the sound IF frequency if the sound carrier is combined with the composite video signal at IF level.

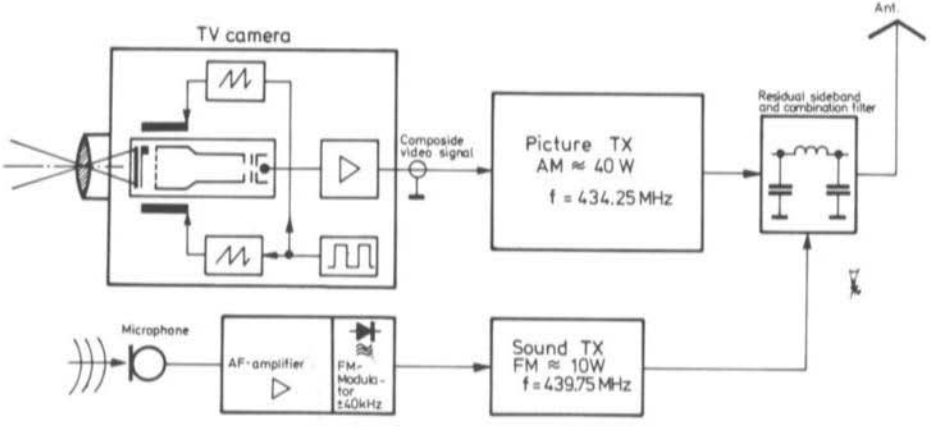

Fig. 6: Block diagram of a typical ATV setup

Figure 6 shows a simplified block diagram of an ATV transmitter using a separate transmitter for the audio and video signals which are combined using a suitable filter in the antenna feeder. This block diagram is to be used to discuss the various modules required for ATV transmissions.

The image to be transmitted is scanned with the aid of the television camera and divided into a large number of individual image points or elements. These points are then converted in the camera tube into corresponding electrical signals which form the basis of the video signal.

Of course, the television camera requires some form of horizontal and vertical deflection in order to be able to scan the light-sensitive signal plate which is perhaps the most important part of the TV camera. These scanning signals are the horizontal and vertical blanking and synchronizing impulses that must be generated in the appropriate circuits within the camera. In order to ensure that the TV receiver is synchronized to the TV camera, it is necessary for these synchronizing signals to be combined with the video information to form the composite video signal.

This composite video signal is modulated onto the video carrier in the video transmitter. Negative amplitude modulation as described in (1) is to be used. The white level corresponds to 10% of the maximum video carrier level and should not be exceeded; otherwise an interference signal will be heard in the sound channel of the TV receiver. The black level corresponds to 75% of the maximum carrier level. The synchronizing pulses are in the so-called blacker-than-black range and obtain the 100% level. An oscilloscope image of the composite video signal (negative AM) is given in Figure 7.

Fig. 7: Picture carrier signal with negative amplitude modulation

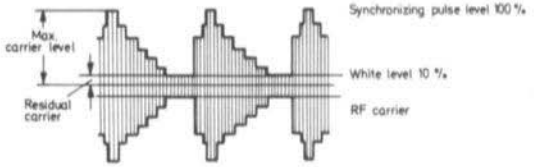

The audio signal in our example represents a conventional frequency modulated 70 cm transmitter of 25% the power of the video transmitter. This FM signal is then fed via a suitable filter to the same antenna as the video signal. This virtually means that two separate 70 cm signals are transmitted using the same antenna.

The other method where the audio and video signals are combined at IF level is to be discussed later in Section 4.4.

4.2. THE TELEVISION CAMERA

Most TV amateurs do not build their own cameras but mainly purchase one of the closed-circuit TV cameras that are available relatively inexpensively on the market. These cameras usually have both an RF and a video output. The author has considered the possibility of using the RF signal, which is usually in TV-Band I, and mixing this up to the required output frequency. However, experience has shown that this RF video signal is not stable enough for this and the TV camera would require modification to obtain sufficient linearity and frequency stability. However, the quality of the video output signal is usually more than sufficient for amateur applications. Of course, the life of the TV camera tube can be spared if test transmissions are made using the video signal from a pattern generator to form a bar or crossbar picture. Such a pattern generator and video pulse center are to be described in VHF COMMUNICATIONS.

Figure 8 gives a simplified block diagram of a closed-circuit TV camera that would be suitable for ATV transmissions. The main parts of the TV camera are the optical system, the signal plate, the camera tube with focusing circuit, the horizontal and vertical deflection coils as well as the deflection circuits where the horizontal and vertical deflection signals are generated. The TV

camera also has circuits which convert the deflection signals required by the camera itself into the blanking and synchronizing pulses that are superimposed on the video signal for synchronization of a monitor, and distant TV receiver. For price reasons, virtually only vidicon and plumbicon TV camera tubes are used in closed-circuit TV cameras. For this reason, the main characteristics of these types of camera tubes is to be examined.

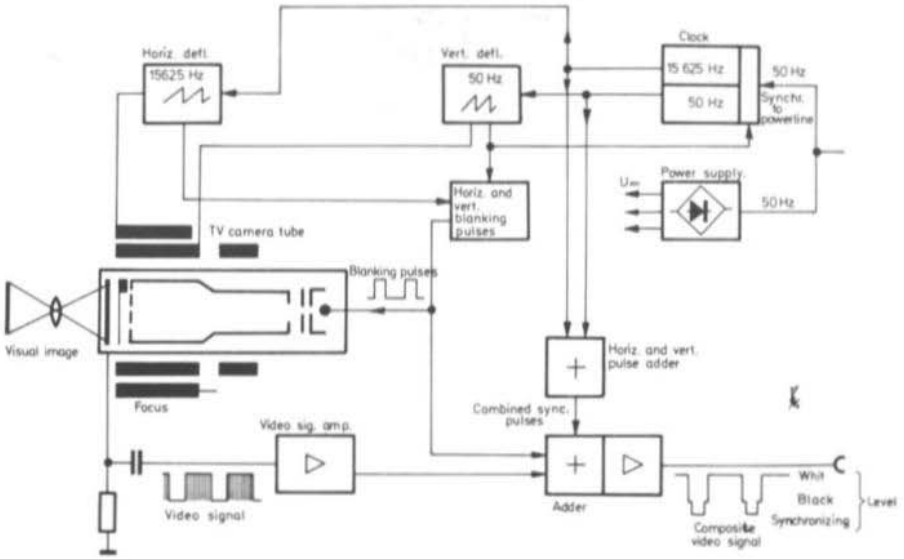

Fig. 8: Block diagram of a TV camera

4.2.1. THE VIDICON CAMERA TUBE

The vidicon camera tube is a charge-storage type comprising the following major parts: Photo-electric (light sensitive) conversion plate, signal plate, and focusing system for obtaining the narrowest possible electronic beam for scanning the signal plate (Fig. 9).

The storage plate of the vidicon comprises a light-sensitive semiconductor layer which is accommodated on a transparent, electrically conductive layer of the signal plate. If light quanta reach the semiconductor layer, the ohmic resistance of this layer will be altered depending on the amount of light due to the photo-electric effect. This means that the difference in the brightness values is accurately mirrored by the difference in the ohmic resistances resulting on the semiconductor layer and that the optical image will have been converted to an electrical image. The transparent, metallic signal plate and the surface of the semiconductor layer also simultaneously form a capacitance whose dielectric is formed by the semiconductor layer.

The equivalent diagram of a single picture element can therefore be represented as the parallel circuit of a capacitance C and an ohmic resistance R (see Fig. 10). The value of the resistance R is dependent on the amount of light present at this point.

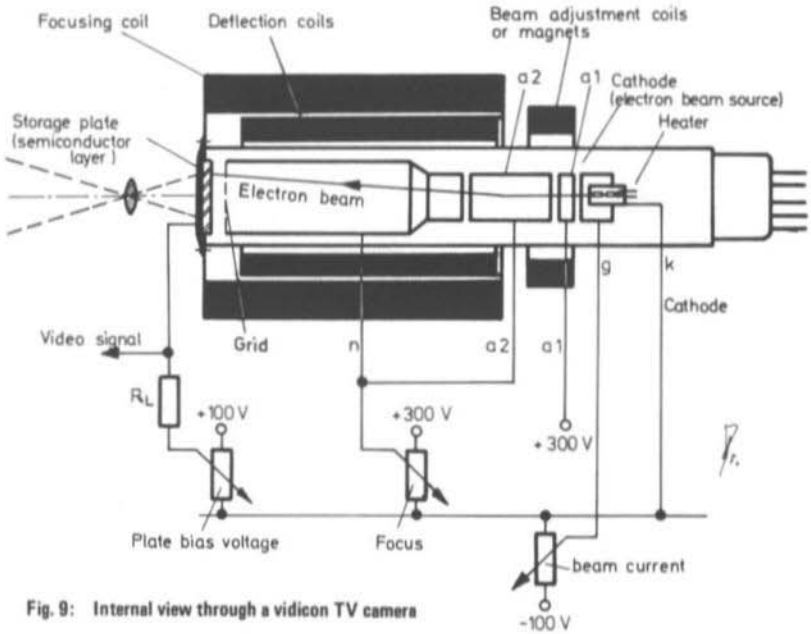

Fig. 9: Internal view through a vidicon TV camera

Each of these individual picture elements is scanned periodically by the electron beam. The electron beam can be said to connect the associated "picture element capacitor" periodically to cathode potential. This "picture element capacitor" can then be discharged via the light-dependent resistor R in the period until the next scan (assuming that the visual image has changed). The periodic scanning of the picture element therefore leads to varying currents that are available as a corresponding voltage across the resistance R_L, which then correspond to the light values present at the individual picture elements on the storage plate.

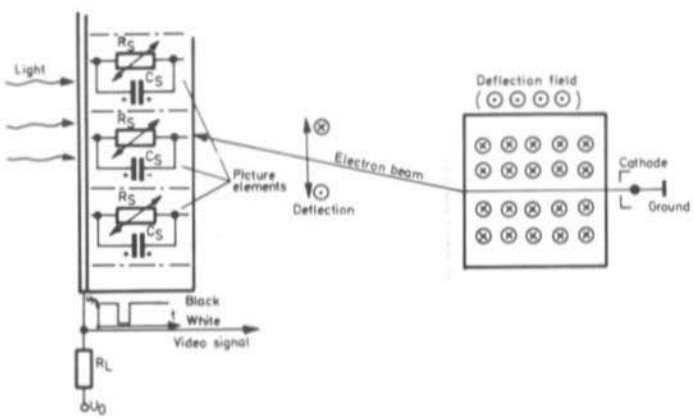

Fig. 10: Principle of the operation of the signal plate

The polarity of the output voltage is negative, e.g. an increase in brightness will cause an increase in current through R_L.

The electron beam system of the camera tube comprises a cathode c, a control electrode g, and anode a 1. Anode a 1 is positive with respect to the cathode so that the electrons are accellerated and pass through an aperture in anode a 2. The voltage of anode a 2 is variable and can be used for electrostatic focusing of the electron beam. However, the voltage on a 2 is usually kept constant and the focusing carried out electro-magnetically using a focusing coil to generate a magnetic field in an axial direction.

Two deflection coils are provided for horizontal and vertical deflection of the electron beam. The required scanning being obtained by passing sawtooth currents of horizontal or vertical frequency respectively through the deflection coils. Some vidicons are available that use electrostatic instead of electromagnetic deflection but they are in the minority.

4.2.2. THE PLUMBICON CAMERA TUBE

The construction and operation of the plumbicon camera tube is very similar to that of the previously described vidicon. The main difference is in the light-sensitive layer which is a lead-oxide layer with the plumbicon and antimony-sulfide in the case of a vidicon. The advantage of the plumbicon is the better non-smearing characteristics (shorter persistence). This also accounts for the price difference between both types. Both tubes are usually graded according to the number of faults (black outs) on the storage plate. This means that it may be possible to obtain reject tubes quite cheaply that are more than sufficient for amateur applications. Generally speaking, the cost of a good vidicon is roughly 60% less than that of a similar quality plumbicon. Both types are decreasing in price due to the popularity of closed-circuit television systems.

4.3. HORIZONTAL AND VERTICAL DEFLECTION; GENERATION OF THE SYNCHRONIZING PULSES

4.3.1. GENERATION OF THE HORIZONTAL SYNCHRONIZATION

The horizontal pulses are usually generated in a multivibrator which is synchronized by a clock. Of course, it is also possible to derive the synchronizing pulses digitally which will be described in detail in conjunction with the ATV pulse center to be described in VHF COMMUNICATIONS. The differentiated squarewave signal from the multivibrator is fed to a single-shot blocking oscillator. The horizontal synchronizing pulse for synchronization of the horizontal deflection stage is taken from the output of the blocking oscillator (Fig. 11). The same pulse is used to control another monostable multivibrator which then generates the horizontal blanking pulse. This pulse is fed to the blanking pulse adder circuit. The horizontal synchronizing pulses are derived from the horizontal multivibrator pulses and their rise slope delayed by approximately 1% with respect to the horizontal blanking pulses.

4.3.2. GENERATION OF THE VERTICAL SYNCHRONIZATION

The vertical pulses are generated in a monostable multivibrator that is synchronized by the power line frequency or a clock (Fig. 11). This pulse is used as vertical blanking pulse and also fed to the blanking pulse adder circuit, which then provides the combined vertical and horizontal blanking signals at the output.

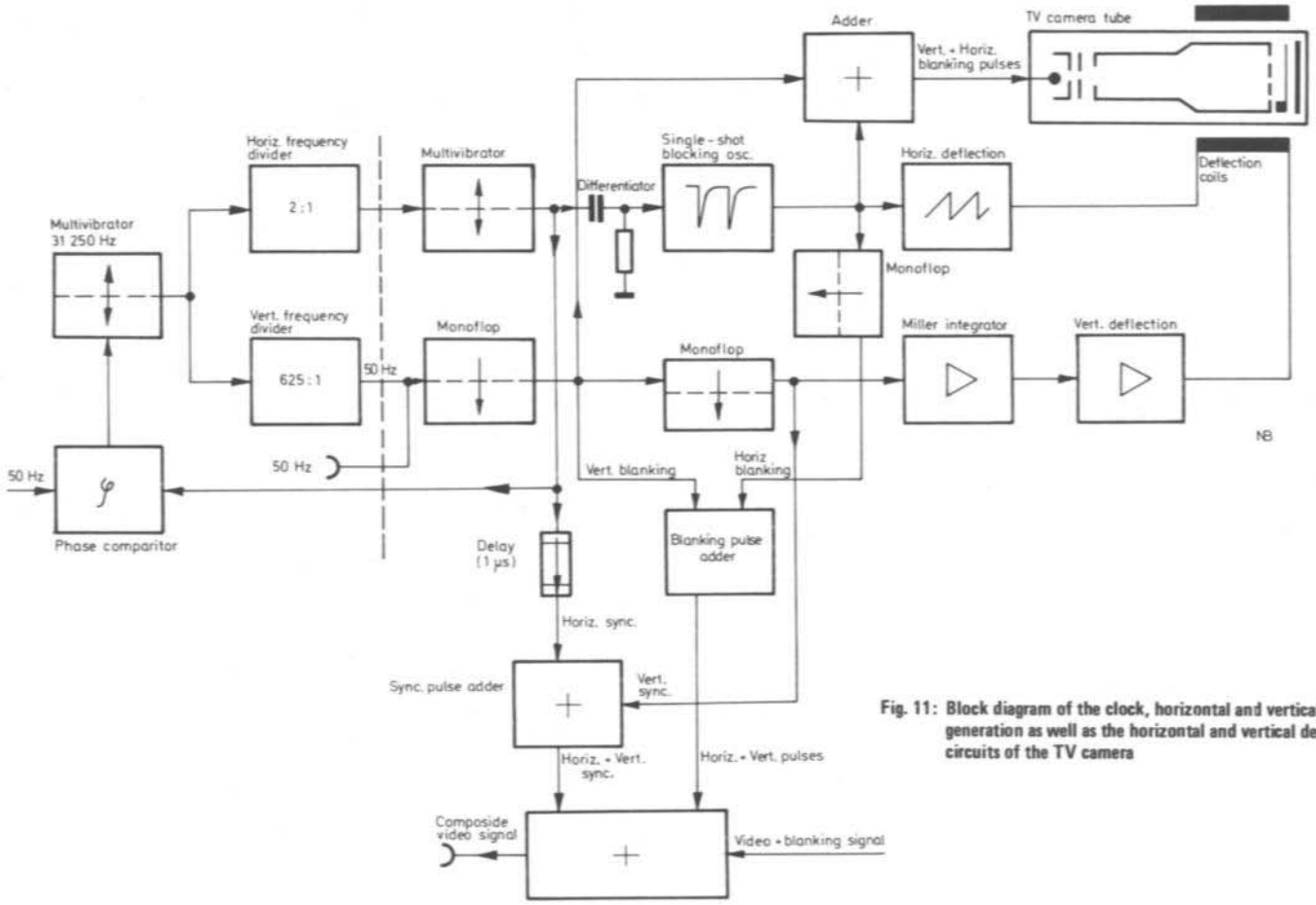

Fig. 11: Block diagram of the clock, horizontal and vertical pulse generation as well as the horizontal and vertical deflection circuits of the TV camera

The vertical synchronizing pulses are generated in a further stage and are also used to drive the vertical deflection circuit. A Miller-integrator is also driven by the vertical synchronizing pulse which provides the sawtooth voltage for the vertical deflection stage.

4.3.3. GENERATION OF THE COMPOSITE VIDEO SIGNAL

The television camera is blanked by the combined vertical and horizontal blanking signal during the retrace period. This means that the combined video and blanking signal is available at the output of the TV camera tube.

The horizontal and vertical synchronizing as well as blanking pulses are added to the amplified video-blanking signal in an adder circuit. A composite video signal of 1 V_{pp} into 75 Ω is usually available at the output of the camera.

4.3.4. THE CLOCK

If higher demands are placed on the synchronization, both deflection circuits should be driven by a clock. This clock consists of a multivibrator that is operative at twice the horizontal frequency, e.g. 31 250 Hz (or from a digital system as previously mentioned). The multivibrator is synchronized by a DC voltage that is derived from the 50 Hz power-line pulses and combined vertical and horizontal pulse after comparison in a phase comparitor.

The horizontal synchronizing pulses are obtained in a 2 : 1 divider whereas the vertical pulses are available at the output of a frequency divider having a total division ratio of 625 : 1. This is obtained by use of four frequency dividers in series each having a division ratio of 5 : 1.

4.4. VIDEO AND AUDIO TRANSMITTERS

4.4.1. VIDEO TRANSMITTER

The construction of the video transmitter mainly depends on whether the modulation (AM) is to be made in the final amplifier (Fig. 12), in the driver stages with subsequent linear amplification or at IF level. As has been previously mentioned, the latter represents the most economical and attractive method technically - at least in the eyes of the author.

If the video information is to be modulated onto the picture carrier in the final amplifier, this will mean that a considerable amount of video energy will be required with a high degree of linearity. Furthermore, the suppression of the lower sideband can only be made after the final amplifier, e.g. at the highest RF level where extensive residual sideband filtering comprising coaxial circuits will be required.

This is another advantage of intermediate frequency modulation in the order of 34 MHz (see Fig. 13). In this case, the picture carrier is mixed or modulated with a fixed intermediate frequency that has already been modulated with the composite video signal. The suppression of the lower sideband is carried out at low level and at lower frequencies where the residual sideband filter can be more efficient and be constructed from lumped components.

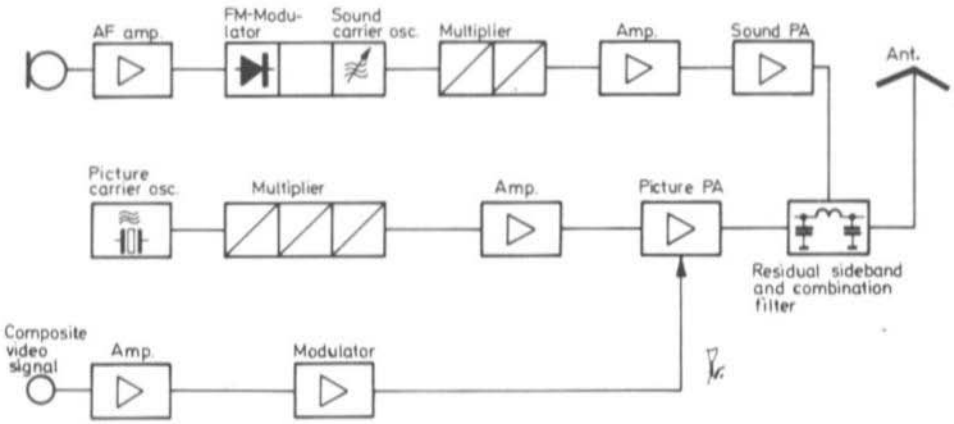

Fig. 12: Block diagram of an ATV transmitter modulated in the PA

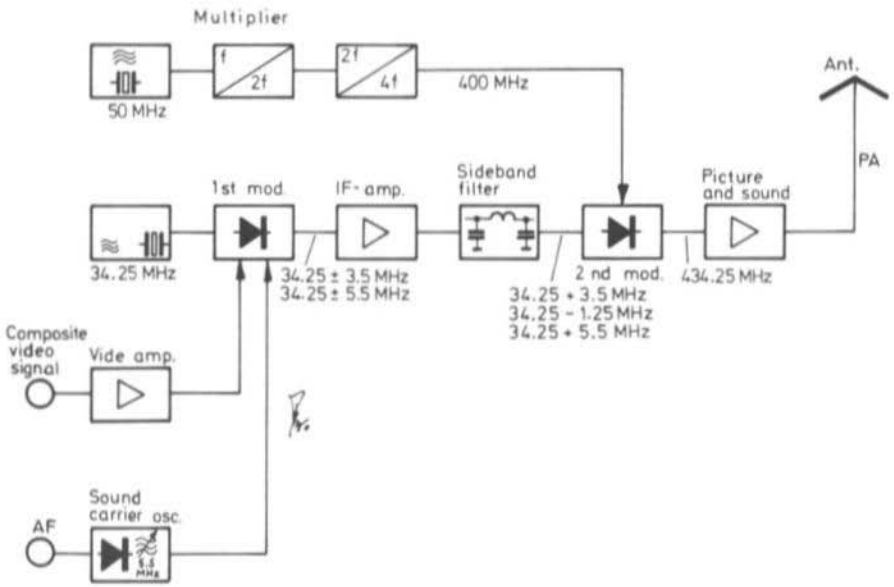

Fig. 13: Block diagram of an ATV transmitter using intermediate frequency modulation

4.4.2. AUDIO TRANSMITTER

The sound carrier is usually transmitted using the same antenna as the picture signal. If a separate audio transmitter is used the sound and picture signals are combined in the antenna feeder using a special filter (Fig. 12). Since such a filter is rather extensive, it is more favourable to modulate the sound carrier onto the picture carrier.

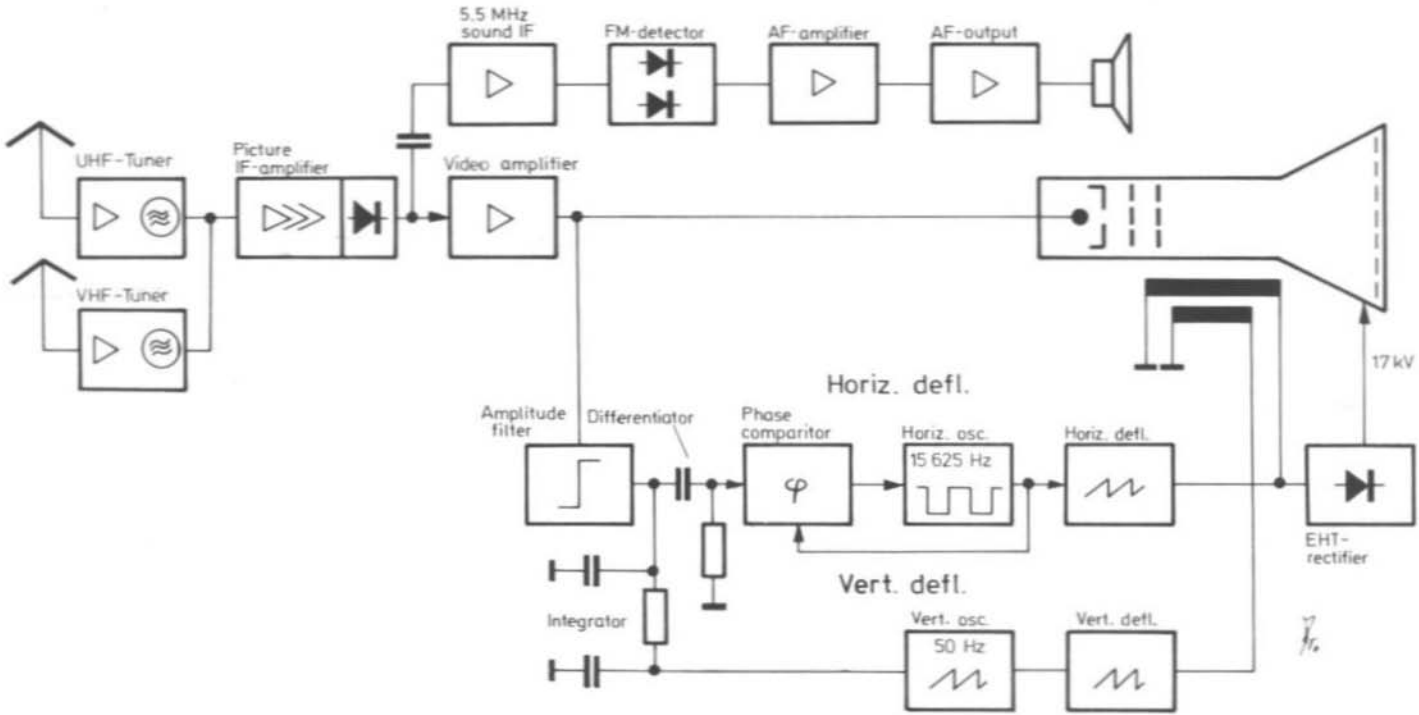

Fig. 14: Simplified block diagram of a monochrome (black and white) television receiver

4.4.3. INTERMEDIATE FREQUENCY MODULATION

In this mode, the composite video signal and the audio signal are not directly modulated onto the picture carrier f_{pc} but onto the modulated intermediate frequency f_{IF}.

After suppression of the lower sideband and appropriate amplification, the intermediate frequency signal is modulated onto the multiplied sub-carrier frequency f_{sc}. The required conversion product is then filtered out and passed via the final amplifier to the antenna.

The actual modulation should always be made at a relatively low immediate frequency in the order of 10 to 50 MHz (in our example 34.25 MHz).

The maximum modulation frequency should not exceed 3.5 MHz which will be completely satisfactory for amateur TV transmissions. Only a very slight deterioration of the picture resolution will be noticed at this bandwidth. An intermediate frequency f_{IF} of 34.25 MHz was selected and the basic frequency of the sub-carrier is 50 MHz. After multiplying the sub-carrier by eight (400 MHz) and adding the intermediate frequency of 34.25 MHz, the resulting picture carrier frequency will be 400 + 34.25 = 434.25 MHz. Both frequencies are generated in crystal oscillators.

5. TELEVISION RECEIVER

Most TV amateurs will no doubt use a domestic television receiver together with a suitable converter or modified UHF-tuner. However, the operation of the television receiver is to be described briefly.

The UHF signal from the antenna is amplified and converted to the IF frequency range (see Fig. 14). The local oscillator frequency is usually above the required frequency which means that the following intermediate frequencies will be obtained:

$f_{IF\ (picture)} = f_{osc} - f_{pc} = 473.15 - 434.25 = 38.9$ MHz

$f_{IF\ (sound)} = f_{osc} - f_{sound} = 473.15 - 439.75 = 33.4$ MHz

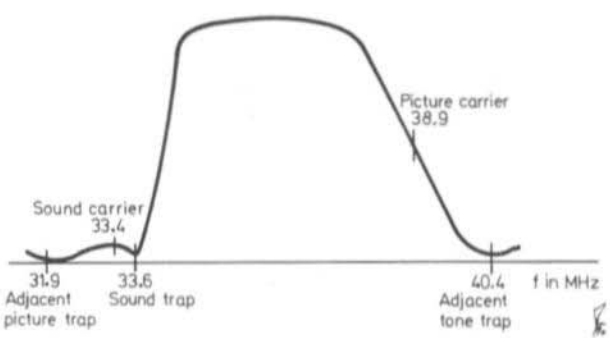

Fig. 15: Passband curve of the picture IF amplifier

These are the normal intermediate frequencies used with receivers operating according to the CCIR standard. These intermediate frequencies are amplified in the video IF amplifier. The passband characteristics of this amplifier are given in Figure 15. The passband curve is reduced to approximately 5% of the maximum IF amplitude at 33.4 MHz using a tone trap aligned to 33.6 MHz.

The amplitude modulated video IF spectrum is detected in the video demodulator in order to obtain the original composite video signal of max. 3.5 MHz. A frequency modulated intercarrier frequency also results at the video demodulator as difference frequency between the sound and picture carriers:

$$f_{IF} = f_{IF\ (picture)} - f_{IF\ (sound)} = 38.9 - 33.4 = 5.5\ MHz$$

The composite video signal is amplified in a video amplifier to an amplitude of between 70 to 100 V_{pp} and fed to the cathode of the picture tube where it controls the electron-beam current.

The frequency modulated 5.5 MHz sound IF is amplified and demodulated in a FM demodulator to form the audio signal which is then amplified and fed to the loudspeaker.

The horizontal and vertical synchronizing pulses are fed to a sync. separator where they are taken from the video signal and fed to a differentiator (horiz.) and integrator (vert.).

The horizontal and vertical sync. pulses are differentiated and compared with the phase of the internal horizontal deflection generator in a phase comparitor circuit. The DC error voltage obtained in this manner is used to keep the horizontal deflection oscillator synchronized to the nominal frequency (derived from the camera or pulse center at the transmit end).

The deflection oscillator also generates the pulses required by the horizontal deflection stage in order to obtain the required deflection of the electron beam in the picture tube.

The extra high tension EHT voltage of approximately 18 kV is obtained by transformation and rectification of the horizontal deflection signal. Many manufacturers have now gone over to voltage multiplication using silicon rod rectifiers (especially with color TV receivers where higher EHT voltages are required).

As has been previously mentioned, the horizontal and vertical pulses are fed to an integrator in order to regain the vertical sync. pulses. This integrator virtually distorts the horizontal pulses so much that they cannot interfere with the vertical synchronization.

The vertical pulses control a vertical oscillator - a multivibrator or blocking oscillator - which together with a charging capacitor generates the control voltage required for the vertical deflection stage.

6. CONCLUSION

The author hopes that this article has brought some insight into the intrigues of amateur television and that it will assist amateurs on their way to becoming active in this mode. VHF COMMUNICATIONS is to bring a number of constructions for the TV amateur including pulse centers, pattern generators and a complete ATV transmitter using the previously mentioned intercarrier principle (IF-level modulation). Such designs will greatly assist amateurs getting active on ATV since they will only require a TV-camera, microphone and a 70 cm antenna.

7. REFERENCES

T. Bittan: Amateur Television
VHF COMMUNICATIONS 4 (1972), Edition 3, Pages 184-190

New AM/FM 2 m Transmitter Module AT 222

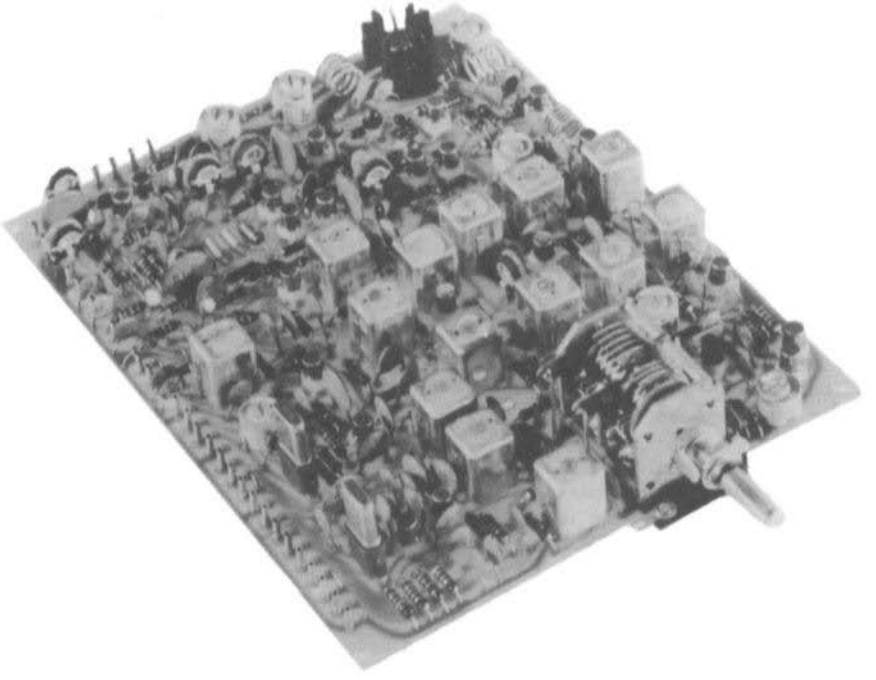

- Switchable to AM and FM
- Built-in synthesis VFO (stability better than 100 Hz/h at 144 MHz) or crystal control
- Built-in speech processor
- Output 1 W FM; 1 W PEP AM
- 12 VDC operation
- Matching linear amplifier for 8 W output available

CRYSTALS and CRYSTAL FILTERS

Crystal filter	XF-9A	(for SSB) with both sideband crystals	DM 110.—
Crystal filter	XF-9B	(for SSB) with both sideband crystals	DM 148.—
Crystal filter	XF-9C	(for AM; 3.75 kHz)	DM 150.—
Crystal Filter	XF-9D	(for AM; 5.00 kHz)	DM 150.—
Crystal filter	XF-9E	(for FM; 12.00 kHz)	DM 150.—
Crystal filter	XF-9M	(for CW; 0.50 kHz) with carrier crystal	DM 110.—
Crystal filter	XF-9NB	(CW filter 8 pole; 400 Hz; w/carrier crystal)	DM 172.—
Crystal filter	QF-9FO	(for FM; 15 kHz)	DM 165.—
Sideband crystal	XF-901	(8.9985 MHz)	DM 15.—
Sideband crystal	XF-902	(9.0015 MHz)	DM 15.—
Carrier crystal	XF-900	(9.0000 MHz)	DM 15.—
Crystal	96.0000 MHz	(HC- 6/U) for 70 cm converters	DM 26.—
Crystal	96.0000 MHz	(HC-25/U) for 70 cm converters	DM 34.—
Crystal	95.8333 MHz	(HC-25/U) for 70 cm converters	DM 34.—
Crystal	78.8580 MHz	(HC- 6/U) for ATV TX (DJ 4 LB)	DM 26.—
Crystal	70.4444 MHz	(HC-25/U) for converter 23 cm / 10 m	DM 26.—
Crystal	67.3333 MHz	(HC- 6/U) for converter 70 cm / 10 m	DM 22.—
Crystal	66.9027 MHz	(HC-25/U) for 24 cm ATV Converter	DM 26.—
Crystal	66.5000 MHz	(HC- 6/U) for synthesis VFO (DJ 5 HD)	DM 22.—
Crystal	65.7500 MHz	(HC- 6/U)	DM 22.—
Crystal	65.5000 MHz	(HC- 6/U) for mixers	DM 22.—
Crystal	65.2500 MHz	(HC- 6/U) 9 MHz / 145 MHz	DM 22.—
Crystal	65.0000 MHz	(HC- 6/U)	DM 22.—
Crystal	64.3333 MHz	(HC- 6/U) for ATV converter (DJ 5 XA)	DM 22.—
Crystal	62.0000 MHz	(HC- 6/U) for synthesis VFO (DJ 5 HD)	DM 22.—
Crystal	57.6000 MHz	(HC-25/U) for converter 70 cm / 2 m	DM 33.50
Crystal	57.6000 MHz	(HC- 6/U) for converter 70 cm / 2 m	DM 22.—
Crystal	45.0690 MHz	(HC-25/U)	DM 24.—
Crystal	45.0080 MHz	(HC-25/U)	DM 24.—
Crystal	44.9600 MHz	(HC-25/U) for RT 33 (DC 3 NT)	DM 24.—
Crystal	44.9170 MHz	(HC-25/U)	DM 24.—
Crystal	44.8080 MHz	(HC-25/U)	DM 24.—
Crystal	38.9000 MHz	(HC- 6/U) for DJ 4 LB 001 ATV-TX	DM 25.—
Crystal	38.6667 MHz	(HC- 6/U) for 2 m converters	DM 17.—
Crystal	1.4400 MHz	(HC- 6/U) for synthesizer DK 1 OF 012	DM 22.50

STANDARD FREQUENCY CRYSTALS

Crystal	5.0000 MHz	(HC- 6/U) for DK 1 OF 022	DM 25.—
Crystal	1.0000 MHz	(XS 6002)	DM 26.—
Crystal	1.0000 MHz	(XS 0605) for 75° ovens	DM 50.—
Crystal oven	XT-2 (12 V)	75°C	DM 82.—
Crystal socket	for HC- 6/U	horizontal mounting	DM 5.—
Crystal socket	for HC-25/U	horizontal mounting	DM 5.—
Crystal socket	for HC-25/U	vertical mounting	DM 1.50
Crystals	72..... MHz	(HC-25/U)	DM 23.—

Following frequencies available as long as stock lasts:
72.000 / 72.025 / 72.050 / 72.100 / 72.125 / 72.150 / 72.175 /
72.200 / 72.225 / 72.250 / 72.275 / 72.300 / 72.325 / 72.350 /
72.375 / 72.400 / 72.425 / 72.450 / 72.475 / 72.500 / 72.575 MHz

Ceramic filter	CFS-455 D	for FM IF-strip DC 6 HL 007	DM 70.—

LINEAR AMPLIFIER FOR 70 cm USING A 2 C 39 TUBE

Further development of the amplifier described in edition 3/72 VHF COMMUNICATIONS

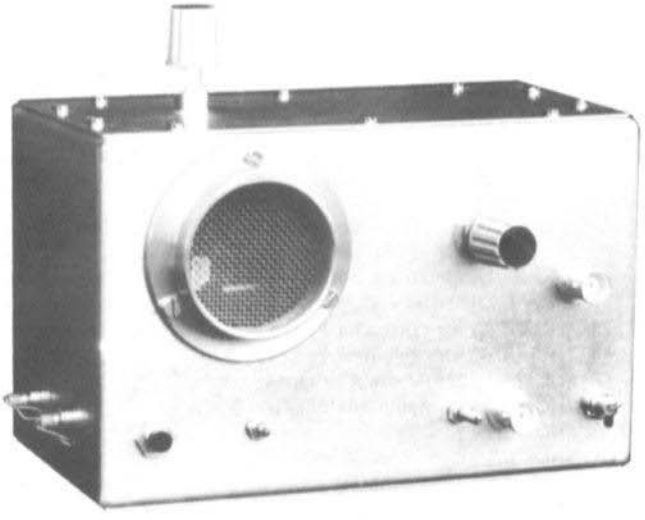

- Silver-plated
- Ready-to-operate
- Supplied without tube, power supply and blower
- Price DM 438,—

INTERDIGITAL BANDPASS FILTER FOR 23 cm

Similar to that described in edition 3/71 VHF COMMUNICATIONS

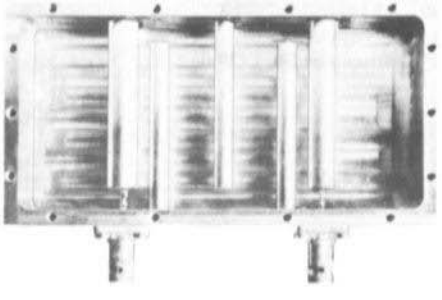

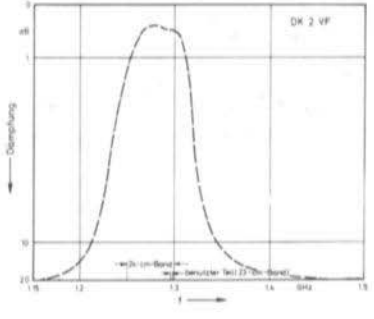

The advantages of interdigital filters is well known: High stopband attenuation and low insertion loss. The curve and insertion loss values are virtually independent of the matching (the filter can be shorted or have an open circuit when an isolation of at least 6 dB exists between this point and the filter).

Price with BNC sockets	DM 92.00
Price without sockets	DM 86.50

STANDARD FREQUENCY OSCILLATOR WITH AN ACCURACY OF 10^{-8}

Ready-to-operate, aged and aligned as described in edition 2/1975 of VHF COMMUNICATIONS

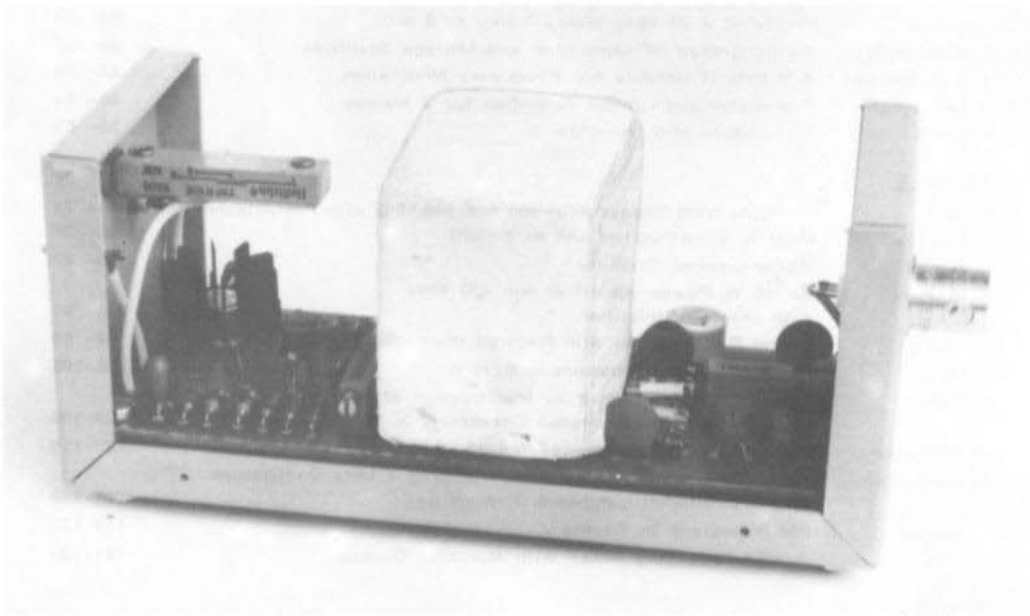

View with cover removed

Frequency:	5 MHz
Crystal:	AT-cut, fundamental
Crystal holder:	HC-36/U
Frequency adjustment:	Mechanical: approx. 3×10^{-5} $\frac{\Delta f}{f}$ Electrical: approx. 1×10^{-6} $\frac{\Delta f}{f}$
Output voltage:	approx. 1 V, sinusoidal
Output impedance:	approx. 200 Ω
Ambient temperature range:	– 20 to + 40°C
Frequency deviation:	
Due to aging:	less than 1×10^{-8} $\frac{\Delta f}{f}$ / day after 24 h period
Due to temperature:	less than 1×10^{-9} $\frac{\Delta f}{f}$ / °C
Due to supply voltage fluctuations of ± 10 % at 18 V:	less than 5×10^{-9} $\frac{\Delta f}{f}$
Due to loading (no-load/short):	less than 1×10^{-8} $\frac{\Delta f}{f}$
Frequency error after switching on at a temperature of 25°C and a supply voltage of 18 V:	
Deviation $\frac{\Delta f}{f}$ from the required frequency:	after 3 min: less than 10^{-6} after 6 min: less than 10^{-7} after 10 min.: less than 10^{-8}
Operating voltage:	+ 14 V to + 28 V to ground
Heating current:	700 to 900 mA
Operating current:	less than 150 mA at 18 V
Dimensions:	125 mm x 55 mm x 55 mm
Weight:	approx. 200 g
Price:	**DM 495.—**

INDEX to VOLUME 4 (1972) of VHF COMMUNICATIONS

Edition 1

G. Otto	Portable SSB Transceiver for 144-146 MHz with FM-Attachment. Part 1: Circuit Description and Specification	2- 15
H. Schotten	Calculations for a Linear VFO	16- 19
D. E. Schmitzer	A Digital Calibration-Spectrum Generator Part 2: 1.001 MHz Accessory and Power Supply	20- 25
E. Ritter	Modifying a 27 MHz Walky-Talky to 2 m	26- 33
D. E. Schmitzer	An Integrated AF-Amplifier and Voltage Stabiliser	34- 39
D. E. Schmitzer	A 9 MHz IF-Module for Frequency Modulation	40- 45
E. Berberich	Transistorized Linear Amplifier for 2 Metres	46- 54
R. Lentz	Circulators and Isolators	55- 60

Edition 2

G. Otto	Portable SSB Transceiver for 144-146 MHz with FM-Attachment. Part 2: Construction and Alignment	66- 79 96- 97
T. Schad	Phase-Locked Circuits	80- 87
K. Hupfer	An 18 W Power Amplifier for 432 MHz with printed Striplines	86- 91
K. Hupfer	23 cm Preamplifier with Printed Micro-Striplines	92- 95
R. Lentz	Circulators and Isolators - Part II	98-102
R. Eide	A 50 MHz Transverter by Modification of Receive Converter DL 6 HA 001 and Transmit Converter DL 6 HA 005	103-106
H. J. Franke	A 12 W DC-DC Converter for 12 V / 28 V	107-110
E. Schmitzer	A 200 kHz Receiver for Synchronizing 1 MHz Oscillators to the Droitwich Longwave Transmitter	111-118
T. Bittan	FM Repeaters in Germany	119-120
R. Lentz	A Wideband Ring Mixer with Schottky Diodes	121-124

Edition 3

W. Schumacher	Dimensioning of Microstripline Circuits	130-143
A. Tautrim	A Stripline Power Amplifier for 70 cm using a 2 C 39 Tube	144-157
G. Otto	Portable SSB Transceiver for 144-146 MHz with FM Attachment. Part III	158-163
R. Griek	Home Made Reflectometer for 100-1400 MHz	164-166
T. Bittan	Recommended Standards for FM Repeaters and Fixed Channel FM Stations in the 2 m Band	167-168
T. Bittan	Modifying the DL 6 HA 001/28 Dual-Gate MOSFET Converter for Reception of Weather Satellites and other Space Vehicles	169-170
G. Rühr	Diplexer Amplifier for 28-30 MHz	171-173
D. E. Schmitzer	List of the Teko Modules already described and Future Additions	174
D. E. Schmitzer	A Crystal Oscillator Module with Three Independent Oscillators	175-179
H. Matuschek	A Simple FET-Tester	180-183
T. Bittan	Amateur Television	184-190

Edition 4

R. L. Harrison	VHF Transequatorial Propagation	194-206
Editors	Corrections and Improvements to the DC 6 HL SSB Transceiver	207
AMSAT Newsl.	OSCAR 6	208-211
H. J. Franke	An Integrated Receiver System for AM, FM, SSB and CW	212-215
W. Schumacher	Dimensioning of Microstripline Circuits - Part 2	216-228
F. Weingärtner	Further Development of the four-digit Frequency Counter	229-234
R. Görl and B. Rössle	A Stable Crystal-Controlled Oscillator in the order of 10^{-7} for Frequency and Time Measurements	235-240
T. Bittan	Amateur Television - Part 2	241-252

High Performance VHF Equipment from

Braun

80 channel 2 meter FM Transceiver SE 280

Immediately ready-for-operation on 80 channels without a single extra crystal. Suitable for operation on any of the standardized FM repeater and simplex frequencies. Covers the whole of the 2 m band in 25 kHz steps. Each of the 80 channels can be selected independently for transmit and receive. Digital frequency selection using frequency synthesis from a 1.25 MHz master crystal. Receiver equipped with a crystal filter and crystal discriminator. Operating voltage is 12 VDC.

A matching AC power supply NT 280 is also available. Completely silicon transistorized with an RCA 2 N 5915 in the PA. Output power is 10 W RF. Insensitive to incorrectly matched antennas. Built-in squelch, 1750 Hz calling tone, and loudspeaker. Connector provided for an external loudspeaker.

SSB/AM/FM/CW 2 meter Transceiver SE 600 digital

A transceiver that really offers you everything. Extremely low noise figure with excellent selectivity, and high cross and intermodulation rejection.

True transceive or separate operation of transmitter and receiver, which can be switched independently to the CW, LSB, USB, AM and FM modes. This versatility allows problemless operation via repeaters, satellite and balloon-carried translators.

Digital frequency readout from the built-in frequency counter using 13 cm Nixie tubes. Direct readout of the transmit and receive frequency; the indication jumps from one to the other on depressing the PTT button etc.

Separate crystal filters for each mode. True AM with plate/screen grid modulation. Built-in speech processor. Product detector for SSB and a crystal discriminator for FM. VOX, antitrip and PTT facilities, as well as RF-output and S-meters. Built-in antenna relay. Built-in power supplies for AC and 12 VDC operation.

SSB/AM/FM/CW 2 meter Transceiver SE 600

This transceiver possesses the same specifications as the SE 600 digital but is equipped with two analog scales. The SE 600 can be equipped with an optional 25 kHz or 50 kHz calibration spectrum generator and calling tone oscillator.

Our manufacturing program also includes 2 m, 6 m, 70 cm converters; 2 m/70 cm varactor triplers and transverters and an active CW filter.

Please request our data sheets

Karl Braun · Communications Equipment

D-85 Nuernberg, Bauvereinstraße 41-45, W. Germany

Representatives:

England: Lowe Electronics, 119 Cavendish Rd, MATLOCK DE 4 3 HE
Holland: Hoogstraal, ALMELO, POB 252
Italy: Radio Meneghel, 31100 TREVISO, Cassella Postale 103

CRYSTAL FILTERS - FILTER CRYSTALS - OSCILLATOR CRYSTALS

SYNONYMOUS for QUALITY and ADVANCED TECHNOLOGY

PRECISION QUARTZ CRYSTALS. ULTRASONIC CRYSTALS.

PIEZO-ELECTRIC PRESSURE TRANSDUCERS

Listed is our well-known series of

9 MHz crystal filters for SSB, AM, FM and CW applications.

In order to simplify matching, the input and output of the filters comprise tuned differential transformers with galvanic connection to the casing.

Filter Type		XF-9A	XF-9B	XF-9C	XF-9D	XF-9E	XF-9M
Application		SSB-Transmit.	SSB	AM	AM	FM	CW
Number of Filter Crystals		5	8	8	8	8	4
Bandwidth (6dB down)		2.5 kHz	2.4 kHz	3.75 kHz	5.0 kHz	12.0 kHz	0.5 kHz
Passband Ripple		< 1 dB	< 2 dB	< 2 dB	< 2 dB	< 2 dB	< 1 dB
Insertion Loss		< 3 dB	< 3.5 dB	< 3.5 dB	< 3.5 dB	< 3 dB	< 5 dB
Input-Output	Z_t	500 Ω	500 Ω	500 Ω	500 Ω	1200 Ω	500 Ω
Termination	C_t	30 pF	30 pF	30 pF	30 pF	30 pF	30 pF
Shape Factor		(6:50 dB) 1.7	(6:60 dB) 1.8	(6:60 dB) 1.8	(6:60 dB) 1.8	(6:60 dB) 1.8	(6: 0 dB) 2.5
			(6:80 dB) 2.2	(6:80 dB) 2.2	(6:80 dB) 2.2	(6:80 dB) 2.2	(6:60 dB) 4.4
Ultimate Attenuation		> 45 dB	> 100 dB	> 100 dB	> 100 dB	>90 dB	> 90 dB

KRISTALLVERARBEITUNG NECKARBISCHOFSHEIM GMBH

D 6924 Neckarbischofsheim · Postfach 7